This article has been accepted for publication in a future issue of this journal, but has not been fully edited. Content may change prior to final publication. Citation information: DOI 10.1109/TVT.2018.2817365, IEEE Transactions on Vehicular Technology

On Multicast Throughput in Multi-hop MIMO Networks with Interference Alignment

Huacheng Zeng, *Member, IEEE,* Xiaoqi Qin, *Member, IEEE,* Xu Yuan, *Member, IEEE,* Feng Tian, *Member, IEEE,* Y. Thomas Hou, *Fellow, IEEE,* Wenjing Lou, *Fellow, IEEE,* Scott F. Midkiff, *Senior Member, IEEE*

***Abstract*—Interference alignment (IA) is widely regarded as a promising interference management technique for wireless networks and its potential is most profound in interference-intensive environments. This motivates us to study IA for multicast communications in multi-hop MIMO networks, which are rich in interference by nature. We develop a set of linear constraints that can characterize a feasible design space of IA for multicast communications. The set of linear constraints constitutes a simple mathematical model of IA that allows us to conduct cross-layer multicast throughput optimization in multi-hop MIMO networks, but without getting involved into the onerous signal design at the physical layer. Based on the mathematical model of IA, we formulate a multicast throughput maximization problem and develop an approximation solution that can achieve $(1-\varepsilon)$-optimality. Simulation results show that the use of IA can significantly increase the multicast throughput in multi-hop MIMO networks and the throughput gain increases with the volume of multicast traffic and the number of antennas.**

***Index Terms*—Multicast communications, interference alignment, MIMO, multi-hop wireless networks.**

I. Introduction

Interference alignment (IA) is a promising technique to manage mutual interference in wireless networks. Since its inception, IA has received much attention in the information theory community and has been widely applied to a wide range of channels and networks (see, e.g., [1]–[3], [5], [10]). The most significant theoretical result of IA so far was developed by Cadambe and Jafar in [1], which showed that the K-user interference channel can achieve $K/2$ degrees of freedom (DoF). This indicates that the total DoFs of the interference channel can increase linearly with the number of users and the total throughput of a wireless network may not be limited by interference. In addition to its theoretical advances, there are also active efforts that are devoted to feasibility validation and performance evaluation of IA in practical networks. For instance, Gollakotta et al. in [2] demonstrated that IA can be applied to WLAN to help increase network throughput significantly. El Ayach et al. in [3] demonstrated experimentally that IA can achieve its theoretical throughput gain in MIMO-OFDM systems.

To date, the benefits of IA has been successfully demonstrated from both theoretical and practical perspectives. A natural question to ask is: in what environment will the benefits of IA be most significant? Based on our observation and understanding, we believe that the potential of IA is most profound in interference-intensive environments. One of such environments is multicast communications, where there are many concurrent multicast groups and each multicast group has one source node and many destination nodes. A large number of links are active simultaneously in this environment, creating a large amount of interference in the network. In addition to being a good environment for IA, multicast is also an important form of communications as it encompasses both unicast and broadcast as its special cases. This motivates us to study IA for multicast communications.

Given that IA in the spatial domain (with MIMO) is most practical, we will focus on the spatial-domain IA in MIMO networks. Within this universe, although there is a large volume of research efforts in the literature, little progress has been made so far for IA for multicast communications in multi-hop MIMO networks (see related work in Section II). This is not surprising, as there exist several technical barriers, which we describe as follows. First, ensuring feasibility of IA for multicast at the physical (PHY) layer is not a trivial problem. By feasibility, we mean that there exist precoding and decoding vectors for each data stream in the network so that it can be transported free of interference. As the construction of precoding and decoding vectors requires complex matrix manipulations, it is not an easy job to ensure IA feasibility, especially in a multi-hop network environment. Second, maintaining tractability (i.e., acceptable complexity) in addition to feasibility brings in another level of challenge. The design of precoding and decoding vectors for each data stream requires complex matrix manipulations, which are notoriously difficult. For networking research, what we need is a simple abstraction of IA capabilities without getting distracted by onerous matrix manipulations. This calls for a simple mathematical model that is provably feasible at the PHY layer. So far such a simple model for multicast IA does not exist. Last but not least, the design of IA for multicast networks is always coupled with MIMO's interference cancellation (IC) and spatial multiplex-

Manuscript received October 26, 2017; revised January 25, 2018; accepted March 13, 2018. This research was supported in part by NSF under grants CNS-1617634, CNS-1642873, CNS-1343222, and CNS-1443889. The work of H. Zeng was partially supported by CNS-1717840 and KSEF-3803-RDE-020. The work of F. Tian was partially supported by the National Natural Science Foundation of China (NSFC) under Grant 61772287.

H. Zeng is with the University of Louisville, Louisville, KY 40292, USA (e-mail: huacheng.zeng@louisville.edu).

X. Qin is with the Beijing University of Posts and Telecommunications, Beijing 100876, China.

X. Yuan is with the University of Louisiana at Lafayette, LA 70504 USA.

F. Tian is with Nanjing University of Posts and Telecommunications, Nanjing 210003, China.

Y. T. Hou, W. Lou, and S. F. Midkiff are with Virginia Tech, Blacksburg, VA 24061 USA.

This article has been accepted for publication in a future issue of this journal, but has not been fully edited. Content may change prior to final publication. Citation information: DOI 10.1109/TVT.2018.2817365, IEEE Transactions on Vehicular Technology

ing (SM), as well as link scheduling in the network. Such a cross-layer design is necessary to maximize the network throughput, but it also introduces significant complexity in problem formulation and solution procedure.

To address these challenges, we propose to classify mutual interferences in the network into two categories: Strong interferences and weak interferences. Strong interferences will be handled by MIMO's IA and IC capabilities and link scheduling, while weak interferences will be simply treated as noise at each receiver. Based on the concept of strong and weak interferences, the contributions of this paper can be summarized as follows:

- We derive a set of linear constraints to characterize a feasible design space of IA for multicast communications in multi-hop MIMO networks. The set of linear constraints constitutes a simple mathematical model of IA that allows us to perform multicast throughput optimization from a networking perspective but without getting involved into onerous signal design at the PHY layer. We show that as long as the set of linear constraints are satisfied, there always exist precoding and decoding vectors at the PHY layer that can support the transportation of all data streams in the network free of strong interferences.
- Based on mathematical model of multicast IA, we develop a set of cross-layer constraints to characterize the interaction of IA, IC, SM, and link scheduling. We formulate a multicast throughput maximization problem to study the impact of IA. For the nonlinear constraints in the formulation, we propose a linearization solution and prove that our linearization solution can achieve $(1-\varepsilon)$-optimality of the original problem.
- We use simulation to study the impact of IA on multicast throughput in multi-hop MIMO networks. Numerical results show that the use of IA can significantly increase multicast throughput. Furthermore, the throughput gain of IA increases with the size of multicast group and the number of multicast sessions.

The remainder of the paper is organized as follows. In Section II, we review related work. In Section III, we develop the system model by presenting a motivating example and characterizing a feasible design space of IA for multicast communications. In Section IV, we formulate a multicast throughput maximization problem to study IA in multi-hop MIMO networks. Section V shows how to linearize the nonlinear constraints in our optimization problem. Section VI presents our simulation results. Section V-C offers discussions and Section VII concludes the paper.

II. Related Work

In the literature, there are an overwhelmingly large number of papers on IA in wireless networks. As this paper studies IA for multicast communications in multi-hop MIMO networks, we focus our literature review on the following two thrusts: (i) IA in multi-hop network, and (ii) multicast in MIMO networks.

IA in multi-hop networks. The concept of IA was coined by Jafar and Shamai for the two-user X channel [5]. The most significant result was developed by Cadambe and Jafar in [1], where they showed that the K-user interference channel could achieve $K/2$ DoFs. Since then, the results of IA have been developed for a variety of channels and networks, such as the K-user MIMO interference channel [6], the X network with arbitrary number of users [7], MIMO channel [3], [4], [8], ergodic capacity in fading channel [9], cellular network [10]–[13], and practical implementations [2], [14].

While there are many papers on IA for single-hop networks from information-theoretic perspective, the advance of IA for multi-hop networks remains scarce. In [15], Li et al. described the idea of IA through several examples to illustrate its benefits. However, the key concept of IA (i.e., aligning the interfering signals from different unintended transmitters to the same direction at each receiver) was not incorporated into their algorithm and was absent in the final solution. In [16], Abdel-Hadi and Vishwanath studied multicast IA for "multihop" single-antenna networks, but "multihop" in their work means two-hop only. It remains unclear how to extend their multicast IA scheme to general multi-hop (more than two hops) networks. In [17], Gou et al. studied IA in a two-hop network, where each node (source, relay, and destination) has two antennas. Due to the special setting, their results cannot be extended to a general multi-hop network. In [18], Zeng et al. developed an IA model for MIMO networks and used the model to solve unicast throughput problem in a multi-hop MIMO network. But their results are limited to unicast traffic. [19] presents a comprehensive study of the challenges and research directions on IA in multi-hop wireless networks.

Muticast in MIMO networks. There is a large body of efforts in the literature that studied multicast communication in multi-hop wireless networks. However, most of them focused on multicast in single-antenna wireless networks. To date, results on multicast in MIMO networks remain limited. In [20], Ge et al. studied multicast communications in both single-antenna and MIMO networks, with the objective of improving multicast throughput and reliability. However, their analysis and proposed multicast transmission scheme were limited to single-hop networks. In [21], Xu et al. proposed an adaptive resource allocation (ARA) scheme for multicast communication in MIMO-OFDM cellular networks. Their ARA scheme was tailored for cellular networks with a base station and multiple users and could not be applied to multi-hop MIMO networks. In [22], Jiang et al. studied a multicast problem in ad hoc MIMO network where a source node attempts to share a streaming message with all nodes in the network via some predefined multi-hop routing tree. They proposed an algorithm to determine the interference-aware scheduling scheme for a set of time slots, with the objective of optimizing the network connectivity. In [23], Rao et al. studied IA in MIMO interference multicast networks under partial channel state information (CSI) feedback, with the aim of minimizing the CSI feedback cost while satisfying IA feasibility constraints with a given DoF requirements. Although these two papers ([22] and [23]) considered interference in multicast MIMO networks, their objectives are different from ours in this paper. In [24], Gao et al. studied a multicast communication problem in a multi-hop MIMO network where each node was equipped

This article has been accepted for publication in a future issue of this journal, but has not been fully edited. Content may change prior to final publication. Citation information: DOI 10.1109/TVT.2018.2817365, IEEE Transactions on Vehicular Technology

TABLE I: Notation.

Constant symbols	
ε	A given approximation error
B	A large constant integer
Φ	The range of strong interference
F	The number of sessions in the network
N	The number of nodes along multicast trees in the network
$\mathcal{N}$	The set of nodes along multicast trees with $\lvert\mathcal{N}\rvert = N$
A	The number of antennas at a node
T	The number of time slots in a frame
W	Network bandwidth
$P_{\rm s}$	The transmit power of an active transmitter
$P_{\rm n}$	The noise power at a receiver
G_{ij}	The gain of the channel between transmitter i and receiver j
S_f	The source node of session f
$\mathcal{D}_f$	The set of destination nodes for session f
$\mathcal{F}_i$	The set of multicast sessions that use node i as a root or an internal node along their multicast tree
$\mathcal{R}_i$	The set of intended receivers of transmitter i
$\mathcal{T}_j$	The set of intended transmitters of receiver j
$\mathcal{P}_j$	The set of nodes that may strongly interfere with node j
$\mathcal{Q}_i$	The set of nodes that may be strongly interfered by node i
$\mathbf{H}_{ji}$	The channel matrix between node j and node i
$\mathbf{u}_i^k$	The precoding vector of the kth stream at transmitter i
$\mathbf{v}_{ij}^k$	The decoding vector at receiver j that is used to decode the kth stream from transmitter $i \in \mathcal{T}_j$
Optimization variables	
$x_i(t)$	$x_i(t)=1$ if node i is transmitter in time slot t and 0 otherwise
$y_i(t)$	$y_i(t)=1$ if node i is receiver in time slot t and 0 otherwise
$r(f)$	The end-to-end data rate of session f
$c_i(t)$	The achievable outgoing rate of node i in time slot t
$c_i^k(t)$	The achievable rate of stream k at node i in time slot t
$p_i^k(t)$	The transmit power for the kth stream at node i in time slot t
$z_i(t)$	The number of outgoing data streams at node i in time slot t
$\lambda_i^k(t)$	The activity of the kth stream at node i in time slot t
$\alpha_{ik}(t)$	The number of interfering streams from node i that to be aligned at node k in time slot t
$\gamma_{ij}^k(t)$	The effective SINR at node j for receiving the kth stream from node i in time slot t
$r_{\min}$	The minimum achievable rate among all multicast sessions

with a cognitive radio (CR). The objective was to minimize the required bandwidth while meeting the throughput requirement of each session. In their work, only MIMO's IC capability was considered while MIMO's IA capability was not explored.

III. System Model

A. A Motivating Example

In MIMO networks, through proper signal design at the transmitter side, multiple interfering signals from different transmitters can be aligned to the same direction at a receiver. As a result, those multiple interfering signals can be canceled by just one DoF. This idea has been demonstrated successfully in a number of prior works (see, e.g., [1]–[3], [10]). We observe that the effectiveness of IA is most profound when (i) the number of interfering signals at a receiver is significant, and (ii) the interfering signals can be aligned into some common directions. A natural question to ask is: in what environment these two conditions are most likely to occur. An answer that comes across naturally is multicast communications, where there are multiple concurrent multicast groups, with each group consisting of multiple users. In what follows, we use an example to illustrate IA in multicast communications. Table I lists the notation that we use in this paper.

Consider the network in Fig. 1, where each node has 2 antennas (DoFs). We use solid arrow line to represent an intended transmission and a dashed arrow line to represent interference in all figures in this paper. In Fig. 1, we have three multicast groups: from N_1 to $\{N_4, N_5\}$, from N_2 to $\{N_4, N_6, N_8\}$, from N_3 to $\{N_7, N_8\}$. For each multicast group, one data stream is sent from the source to its destination nodes. We assume that the interference from N_1 to N_8 and from N_3 to N_4 is negligible due to the long distance path loss. Among the five receivers, N_5, N_6, and N_7 receive one desired data stream and two interfering streams as shown in the figure. Without using IA, the desired data stream at N_5, N_6, and N_7 cannot be decoded free of interference, due to the existence of two interfering streams.

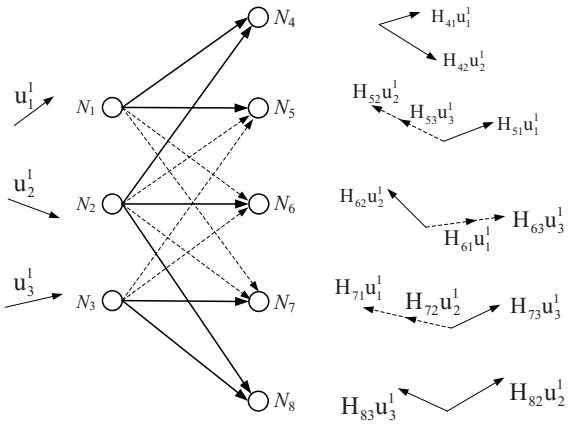

Fig. 1: An example that illustrates IA for multicast.

To show how IA makes it possible to send three data streams in the three multicast groups, we design precoding vectors for the three transmitters (N_1, N_2, and N_3) as follows:

$$\begin{aligned} \mathbf{u}_1^1 &:= \text{eigvec}(\mathbf{H}_{61}^{-1}\mathbf{H}_{63}\mathbf{H}_{53}^{-1}\mathbf{H}_{52}\mathbf{H}_{72}^{-1}\mathbf{H}_{71}) \,, \\ \mathbf{u}_2^1 &:= \mathbf{H}_{72}^{-1}\mathbf{H}_{71}\mathbf{u}_1^1 \,, \\ \mathbf{u}_3^1 &:= \mathbf{H}_{63}^{-1}\mathbf{H}_{61}\mathbf{u}_1^1 \,, \end{aligned} \tag{1}$$

where $\mathbf{u}_i^k$ is the precoding vector of the kth transmitted data stream at node N_i ($i = 1, 2, 3$); $\mathbf{H}_{ji}$ is the channel matrix between node j and node i, which is assumed to have full rank throughout the paper; $\text{eigvec}(\mathbf{H})$ is an eigenvector of square matrix $\mathbf{H}$; and operation ":=" means that two nonzero vectors are in the same direction, that is, $\mathbf{u}_1 := \mathbf{u}_2$ if and only if there exists a nonzero complex number a such that $\mathbf{u}_1 = a\mathbf{u}_2$.

By using the above precoding vectors at transmitters N_1, N_2, and N_3, we have the following observations on the interference at receivers N_5, N_6, and N_7. At receiver N_5, the interference from N_2 is in the direction of $\mathbf{H}_{52}\mathbf{u}_2^1$ and the interference from N_3 is in the direction of $\mathbf{H}_{53}\mathbf{u}_3^1$. It is easy to check that these two interferences now align to the same direction (i.e., $\mathbf{H}_{52}\mathbf{u}_2^1 := \mathbf{H}_{53}\mathbf{u}_3^1$). Similarly, at receiver N_6, we can verify that the interferences from N_1 and N_3 are aligned to the same direction, i.e., $\mathbf{H}_{61}\mathbf{u}_1^1 := \mathbf{H}_{63}\mathbf{u}_3^1$. Finally, at receiver N_7, we can verify that the two interfering streams from N_1 and N_2 are aligned to the same direction (i.e., $\mathbf{H}_{72}\mathbf{u}_2^1 := \mathbf{H}_{71}\mathbf{u}_1^1$). In summary, Fig. 1 shows the IA scheme resulting from the precoding vectors in (1), where the two interfering streams at receivers N_5, N_6, and N_7 are successfully aligned to the same direction.

This article has been accepted for publication in a future issue of this journal, but has not been fully edited. Content may change prior to final publication. Citation information: DOI 10.1109/TVT.2018.2817365, IEEE Transactions on Vehicular Technology

With the precoding vectors in (1), we now show that the desired data streams can be decoded free of interference at each receiver (i.e., N_4, N_5, N_6, N_7, and N_8). Denote $\mathbf{v}_{ij}^k$ as the decoding vector at node j to decode the kth data stream from node i. In this example, receivers N_5, N_6, and N_7 have one decoding vector while receivers N_4 and N_8 have two decoding vectors. To decode the desired data streams at each receiver, we use the following decoding vectors:

$$\begin{array}{l}(\mathbf{v}_{14}^1)^T := [1\ 0][\mathbf{H}_{41}\mathbf{u}_1^1\ \mathbf{H}_{42}\mathbf{u}_2^1]^{-1}\ ;\\ (\mathbf{v}_{24}^2)^T := [0\ 1][\mathbf{H}_{41}\mathbf{u}_1^1\ \mathbf{H}_{42}\mathbf{u}_2^1]^{-1}\ ;\\ (\mathbf{v}_{15}^1)^T := [1\ 0][\mathbf{H}_{51}\mathbf{u}_1^1\ \mathbf{H}_{52}\mathbf{u}_2^1]^{-1}\ ;\\ (\mathbf{v}_{26}^1)^T := [0\ 1][\mathbf{H}_{61}\mathbf{u}_1^1\ \mathbf{H}_{62}\mathbf{u}_2^1]^{-1}\ ;\\ (\mathbf{v}_{37}^1)^T := [0\ 1][\mathbf{H}_{71}\mathbf{u}_1^1\ \mathbf{H}_{73}\mathbf{u}_3^1]^{-1}\ ;\\ (\mathbf{v}_{28}^1)^T := [1\ 0][\mathbf{H}_{82}\mathbf{u}_2^1\ \mathbf{H}_{83}\mathbf{u}_3^1]^{-1}\ ;\\ (\mathbf{v}_{38}^2)^T := [0\ 1][\mathbf{H}_{82}\mathbf{u}_2^1\ \mathbf{H}_{83}\mathbf{u}_3^1]^{-1}\ .\end{array} \tag{2}$$

We now characterize the relationship between the precoding vectors in (1) and the decoding vectors in (2). Through simple manipulation, it is easy to verify that the constructed precoding and decoding vectors satisfy the zero-forcing IC requirements:

$$(\mathbf{v}_{i'j}^{k'})^T\mathbf{H}_{ji}\mathbf{u}_i^k = \begin{cases} 1 & \text{if } \mathbf{v}_{i'j}^{k'} \text{ is designed for the data stream,} \\ & \text{of } \mathbf{u}_i^k, \text{ i.e., } (i',k') = (i,k), \\ 0 & \text{otherwise.}\end{cases}$$

Therefore, by using IA, three data streams can be sent to their respective multicast groups free of interference.

B. Characterizing Feasible Design Space

In the motivating example, we demonstrated that a proper design of precoding vectors at the transmitters can align the interfering signals from different transmitters to the same direction at each receiver. But we did not explain how to design those precoding vectors. In what follows, we establish the connection between the design of precoding vectors and a feasible IA design space defined by a set of simple constraints. We will show that as long as an IA scheme falls in the space defined by a set of simple constraints, such an IA scheme is always achievable at the PHY layer through a proper design of precoding vectors.

Consider a multi-hop multicast network in Fig. 2(a). Each node has the same number of antennas, which we denote as A. Among the nodes, there are a set of multicast sessions. Each session's multicast tree is computed through some multicast routing protocol (e.g., Open Shortest Path First protocol or OSPF protocol [25]). Denote $\mathcal{N}$ as the set of nodes associated with the multicast routing trees, with N being its cardinality (i.e., $N = |\mathcal{N}|$). Assuming transmission scheduling is done within a time frame consisting of T time slots. Within one time slot, only a subset of nodes may be active due to half-duplex and interference constraints. Among the active nodes, a transmit node may send its data to multiple receive nodes (in one-hop multicast branch) simultaneously, as shown in Fig. 2(b).

Strong Interference vs. Weak Interference. Referring to Fig. 2(b), for a receiver in a time slot (see, e.g., N_3), it is being interfered by all its unintended transmit nodes in the network. Interferences from different nodes have different strengths at receive node N_3. Those interfering nodes that are closer to node N_3 will have stronger interference on N_3 than those that are far away. To distinguish such difference, we classify the interferences at a receiver into two groups: *strong interferences* and *weak interferences.* For strong interferences, we will nullify them using MIMO's IA and IC capabilities (zero-forcing). For weak interferences, we will simply treat them as noise.

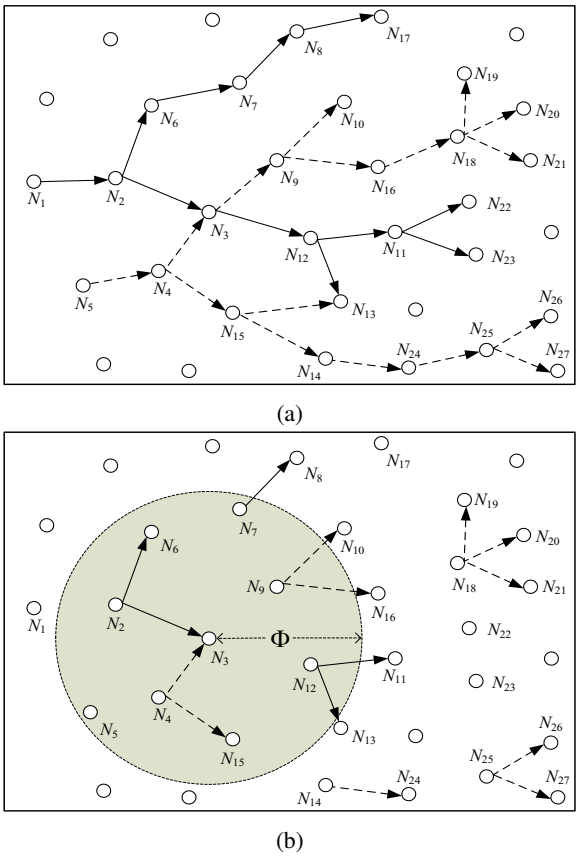

Fig. 2: An example of multicast communications in a multi-hop wireless network. In (a), there are 2 multicast sessions: from source N_1 to multicast group $\{N_{13}, N_{17}, N_{22}, N_{23}\}$, and from source N_5 to multicast group $\{N_{10}, N_{13}, N_{14}, N_{19}, N_{20}, N_{21}, N_{26}, N_{27}\}$. In (b), a set of active transmitters and receivers in time slot t corresponding to the two multicast sessions. The gray disk centered at N_3 is used to classify strong and weak interferences on node N_3.

The next question is: how do we classify an interference as strong or weak interference at a receive node? An accurate approach is to classify an interference based on its strength at its receiving node. However, the strength-based approach requires both large-scale (path loss and shadow fading) and small-scale (fast fading) channel information, which may not be available at a receiver. Therefore, in this paper, we employ a coarse approach by defining an interference range, which is denoted as Φ. If the interfering transmitter is within a radius of Φ from the receiver, then the interference is considered as a strong interference. Otherwise, the interference is considered as a weak interference. For example, for receive node N_3 in

This article has been accepted for publication in a future issue of this journal, but has not been fully edited. Content may change prior to final publication. Citation information: DOI 10.1109/TVT.2018.2817365, IEEE Transactions on Vehicular Technology

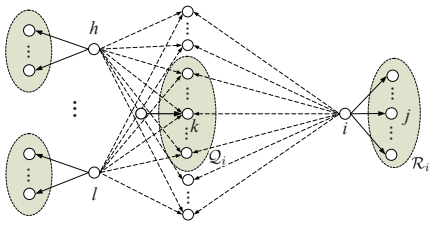

Fig. 3: An illustration of multicast IA constraints at transmit node i. The intended transmitter of receive node k is not shown.

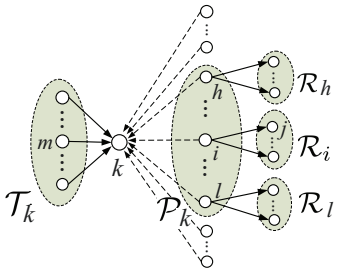

Fig. 4: An illustration of multicast IA constraints and DoF consumption constraints at receive node k.

Fig. 2(b), the interferences from the transmitters within the shadowed area (e.g., N_7, N_9, and N_{12}) are considered as strong interferences, while the interferences from the transmitters outside the disk (e.g., N_{14}, N_{18}, and N_{25}) are considered as weak interferences. Obviously, the setting of interference range Φ is critical. A similar problem has been explored by Shi et al. in [29], which gave a guideline on the optimal setting of interference range. In Section VI, we will also explore the optimal setting of Φ for multicast IA via numerical results.

Multicast IA Constraints: Transmitter Side. Consider a transmit node in time slot t, say node i, in a multicast network as shown in Fig. 2(a). For ease of explanation, we show transmit node i and its neighboring nodes in Fig. 3. Denote $z_i(t)$ as the number of outgoing data streams from transmit node i. Denote $\mathcal{R}_i$ as the set of node i's immediate next-hop nodes along i's downstream multicast tree(s). For example, for node N_2 in Fig. 2(a), we have $\mathcal{R}_2 = \{N_3, N_6\}$. For receive nodes in $\mathcal{R}_i$, we should ensure that all of them can receive the data from transmit node i successfully.[1] Based on interference range Φ, denote $\mathcal{Q}_i$ as the set of nodes that are strongly interfered by transmit node i (see Fig. 3). Receive nodes outside $\mathcal{Q}_i$ are therefore considered to be weakly interfered by transmit node i.

We now consider a receive node $k \in \mathcal{Q}_i$ in Fig. 3. It is interfered by $z_i(t)$ streams from transmit node i. It is also interfered by the interfering streams from some other unintended transmitters (e.g., transmitters h and l in Fig. 3). As demonstrated in Section III-A, through a proper design of the precoding vectors at transmit node i, we can align some (or all) of these $z_i(t)$ interfering streams to other interfering streams (e.g., from h and l) at receive node k. Among these $z_i(t)$ interfering streams, denote $\alpha_{ik}(t)$ as the number of interfering streams that can be successfully aligned to other interfering streams (e.g., from h and l) at receive node k. Then, at receive node k, the number of "effective" interfering streams from transmit node i is reduced from $z_i(t)$ to $z_i(t) - \alpha_{ik}(t)$. Note that variable $\alpha_{ik}(t)$ characterizes the IA space for the $z_i(t)$ interfering streams from transmit node i to receive node k. A larger value of $\alpha_{ik}(t)$ means that more interfering streams from transmit node i can be successfully aligned to other interfering streams at receive node k. Next, we derive constraints for α_{ik} to characterize the design space of IA at transmit node i.

Referring to Fig. 3, let's consider one of the outgoing stream at transmit node i and its precoding vector, say $\mathbf{u}_i^1$. This outgoing stream will strongly interfere all the receive nodes in $\mathcal{Q}_i$. At receive node $k \in \mathcal{Q}_i$, the direction of this interfering stream is $\mathbf{H}_{ki}\mathbf{u}_i^1$. By properly constructing $\mathbf{u}_i^1$, we can align this interfering stream to any particular direction at receive node k. Suppose that $\mathbf{u}_i^1$ is constructed to align this interfering stream to a particular direction at receive node k. Then, at the receive nodes in $\mathcal{Q}_i \backslash \{k\}$, the direction of this interfering stream is also fixed and has no freedom for alignment. This indicates that the construction of a precoding vector can only guarantee one of its corresponding interfering streams to be successfully aligned (at one receive node). Since there are $z_i(t)$ precoding vectors at transmit node i, we can align $z_i(t)$ interfering streams to any directions among the receive nodes in $\mathcal{Q}_i$. That is, there are at least $z_i(t)$ interfering streams from transmit node i that can be aligned to any particular directions. Therefore, a sufficient condition of $\alpha_{ik}(t)$ for $k \in \mathcal{Q}_i$ can be written as:

$$\sum_{k \in \mathcal{Q}_i} \alpha_{ik}(t) \leq z_i(t), \qquad 1 \leq i \leq N, 1 \leq t \leq T. \tag{3}$$

Multicast IA Constraints: Receiver Side. We now consider a receive node in time slot t, say k, in a multicast network as shown in Fig. 2(a). Similarly, for ease of explanation, we show receive node k and its neighboring nodes in Fig. 4. Denote $\mathcal{P}_k$ as the set of nodes that may strongly interfere receive node k (e.g., nodes i, h, and l in Fig. 4). Transmit nodes outside $\mathcal{P}_k$ are considered to be weak interferer and their interferences will be treated as noise at receive node k. Among the $z_i(t)$ interfering streams from transmit node $i \in \mathcal{P}_k$, constraint (3) ensures that α_{ik} interfering streams can be aligned to any directions at receive node k. However, to ensure the resolvability of the data streams at the receive nodes in $\mathcal{R}_i$, any two interfering streams from transmit node i cannot be aligned to the same direction.[2] The following lemma offers a sufficient condition to ensure that any two interfering streams from transmit node i will not be aligned to the same direction at receive node k:

[1] Note that multicast communication differs from multi-user MIMO communication. In multicast communication, every receive node in $\mathcal{R}_i$ will receive the same (all) outgoing data streams from transmit node i. In contrast, in multi-user MIMO, each node in $\mathcal{R}_i$ will receive different subset of outgoing data streams from node i and consider the rest as interference.

[2] The details are explained in the proof of Theorem 1 in Appendix B.

This article has been accepted for publication in a future issue of this journal, but has not been fully edited. Content may change prior to final publication. Citation information: DOI 10.1109/TVT.2018.2817365, IEEE Transactions on Vehicular Technology

Lemma 1: For a receive node k, if

$$\alpha_{ik}(t) \leq \sum_{h \in \mathcal{P}_k}^{h \neq i} [z_h(t) - \alpha_{hk}(t)], \quad 1 \leq k \leq N, i \in \mathcal{P}_k, 1 \leq t \leq T \ , \tag{4}$$

then there exists an IA scheme where any two interfering streams from transmit node $i \in \mathcal{P}_k$ are not aligned to the same direction at receive node k.

In (4), the left hand side (LHS) is the number of "alignable" interfering streams from transmit node i; and the right hand side (RHS) is the number of directions occupied by the interference from the transmit nodes in $\mathcal{P}_k$ other than transmit node i. Lemma 1 says that, at receive node k, if the "alignable" interfering streams from transmit node i are no more than the directions occupied by the interference from the transmit nodes in $\mathcal{P}_k \backslash \{i\}$, then every two interfering streams from transmit node $i \in \mathcal{P}_k$ will not be aligned to the same direction. The proof of this lemma is given in Appendix A.

DoF Consumption Constraints. Constraints (3) and (4) characterize how many interfering streams can be successfully aligned for each interfering node pair (i, k). Based on (3) and (4), we derive the constraints to characterize how many data streams at each transmitter can be successfully transported to their receiver(s). In a time slot t, a node can be a transmitter, a receiver, or idle. For a node $k \in \mathcal{N}$, we define a binary variable $y_k(t)$ to indicate whether or not node k is a receiver in time slot t. Specifically, $y_k(t) = 1$ if node k is a receiver in time slot t and 0 otherwise. If node k is a receiver, then it may have multiple incoming links (e.g., N_3 in Fig. 2) as it may be on multiple multicast trees. Denote $\mathcal{T}_k$ as the set of node k's one-hop upstream nodes along all the multicast trees. For example, for N_3 in Fig. 2(a), we have $\mathcal{T}_3 = \{N_2, N_4\}$. Then we have the following observations on the desired data streams and interfering streams at node k:

- *Node k is a receiver in time slot t, i.e., $y_k(t) = 1$.* In this case, as shown in Fig. 4, node k receives $z_m(t)$ data streams from node $m \in \mathcal{T}_k$ and $z_i(t)$ interfering streams from node $i \in \mathcal{P}_k$. Based on (3) and (4), the $z_i(t)$ interfering streams from node $i \in \mathcal{P}_k$ occupy $z_i(t) - \alpha_{ik}(t)$ new directions at node k because $\alpha_{ik}(t)$ interfering streams have been successfully aligned to other interfering streams at node k. Therefore, to ensure the DoF consumption constraint at node k is satisfied, we must have: $\sum_{m \in \mathcal{T}_k} z_m(t) + \sum_{i \in \mathcal{P}_k} [z_k(t) - \alpha_{ik}(t)] \leq A$.
- *Node k is not a receiver in time slot t, i.e., $y_k(t) = 0$.* In this case, node k does not have any desired data streams from node $m \in \mathcal{T}_k$. So there is no restriction on the number of effective interfering directions at node k. That is, we should not impose any upper bound on $\sum_{i \in \mathcal{P}_k} [z_k(t) - \alpha_{ik}(t)]$.

Combining these two cases, we have

$$\sum_{m \in \mathcal{T}_k} z_m(t) + \sum_{i \in \mathcal{P}_k} [z_i(t) - \alpha_{ik}(t)] \leq A + [1 - y_k(t)] \cdot B, \quad 1 \leq k \leq N, 1 \leq t \leq T, \tag{5}$$

where B is a large enough constant (e.g., $B = N \cdot A$) that can be used as a loose upper bound for $\sum_{i \in \mathcal{P}_k} [z_i(t) - \alpha_{ik}(t)]$. In (5), the first left-hand side (LHS) term $\sum_{m \in \mathcal{T}_k} z_m(t)$ is the number of data streams that need to be decoded at receiver k. This term corresponds to MIMO's spatial multiplexing (SM) capability at receiver k. The second LHS term $\sum_{i \in \mathcal{P}_k} [z_i(t) - \alpha_{ik}(t)]$ is the number of interfering data streams that need to be canceled at receiver k. This term corresponds to MIMO's IC capability at receiver k. Particularly, in this term, "$\alpha_{ik}(t)$" is the number of interfering streams that have been successfully aligned, which reflects the effect of IA.

Summary. Collectively, constraints (3)–(5) characterize a feasible IA space for a multicast network in a time slot. Note that these three constraints are linear and only require simple integer addition and subtraction operations. By using these constraints, we can avoid computing those complex precoding vectors at the PHY layer while still ensuring that our results are feasible. This is a significant advantage, and lays the foundation for our investigation of multicast IA in multi-hop wireless networks. We summarize our discussions with the following theorem:

Theorem 1: If constraints (3), (4), and (5) are satisfied, then there exist precoding and decoding vectors at the PHY layer such that each transmit node i can send $z_i(t)$ data streams to its one-hop multicast receive nodes in $\mathcal{R}_i$ free of strong interference.

The proof of Theorem 1 is presented in Appendix B.

IV. Problem Formulation

Constraints (3), (4), and (5) in the previous section constitute a simple mathematical model of IA that allows us to study cross-layer multicast throughput optimization problem in multi-hop MIMO networks, but without getting involved into the onerous signal design at the PHY layer. Based on the feasible space defined by (3), (4), and (5), we study a multicast throughput maximization problem.

Consider a multi-hop MIMO network consisting of a set of nodes as shown in Fig. 2(a). Each node in the network has the same number of antennas, which we denote as A. Among the nodes there are F multicast sessions. For each session f, it has one source node (denoted as S_f), a set of intermediate nodes, and a group of destination nodes (denoted as set $\mathcal{D}_f$). We assume each multicast tree is computed based on some multicast routing protocol (e.g., OSPF [25]). Denote $r(f)$ as the achievable end-to-end data rate of multicast session f. Denote $r_{\min}$ as the minimum achievable end-to-end data rate among all sessions, i.e., $r_{\min} = \min_{1 \leq f \leq F}\{r(f)\}$. Our objective is to maximize the minimum achievable end-to-end data rate ($r_{\min}$) among all sessions.[3] In what follows, we will focus on the mathematical underpinning of maximizing the minimum achievable end-to-end data rate.

Multicast Node Constraints. Denote $x_i(t)$ as a binary variable to indicate whether or not node $i \in \mathcal{N}$ is a transmitter in time slot t. Specifically, $x_i(t) = 1$ if node i is a transmitter in time slot t and 0 otherwise. Recall that $y_i(t)$ is a binary variable to indicate whether or not node i is a receiver in time

[3]Problems with other objectives such as maximizing sum of weighted rates or a proportional increase (scaling factor) of all session rates belongs to the same category and can be solved following the same token.

This article has been accepted for publication in a future issue of this journal, but has not been fully edited. Content may change prior to final publication. Citation information: DOI 10.1109/TVT.2018.2817365, IEEE Transactions on Vehicular Technology

slot t. For each node, we assume that it has a half duplex radio.[4] That is, a node cannot be a transmitter and a receiver in the same time slot. Then we have:

$$x_i(t) + y_i(t) \le 1, \quad 1 \le i \le N, 1 \le t \le T. \tag{6}$$

Consider a node $i \in \mathcal{N}$ in time slot t. If it is a transmitter (i.e., $x_i(t) = 1$), then there is at least one outgoing data stream at node i, i.e., $z_i(t) \ge 1$. Otherwise (i.e., $x_i(t) = 0$), there are no outgoing data streams at node i, i.e., $z_i(t) = 0$. Combining these two cases, we have

$$x_i(t) \le z_i(t) \le A \cdot x_i(t), \quad 1 \le i \le N, 1 \le t \le T\,. \tag{7}$$

In time slot t, if $x_i(t) = 1$ (i.e., node $i \in \mathcal{N}$ is a transmitter), then each of its next-hop nodes in $\mathcal{R}_i$ (see Fig. 3) should be a receiver, i.e., $y_j(t) = 1$ for $j \in \mathcal{R}_i$. Otherwise (i.e., $x_i(t) = 0$), $y_j(t)$ can be either 0 or 1 for $j \in \mathcal{R}_i$, i.e., no restriction on $y_j(t)$. Combining these two cases, we have

$$x_i(t) \le y_j(t), \quad 1 \le i \le N, j \in \mathcal{R}_i, 1 \le t \le T\,. \tag{8}$$

One-Hop Multicast Rate Constraints. At node i, there are $z_i(t)$ outgoing data streams. If node i is not a transmitter, then $z_i(t) = 0$. Denote $P_{\rm s}$ as the total transmit power of all outgoing data streams at node i. We assume $P_{\rm s}$ is the same for all transmit nodes. Among the $z_i(t)$ outgoing data streams at node i, we denote p_i^k as the transmit power that is allocated to its kth outgoing data stream. Then we have

$$\sum_{k=1}^{z_i(t)} p_i^k(t) = P_{\rm s} \cdot x_i(t), \quad 1 \le i \le N, 1 \le t \le T\,. \tag{9}$$

Referring to Fig. 3, consider one-hop multicast data transmission from transmit node i and the receive nodes in $\mathcal{R}_i$. Due to wireless multicast advantage, the transmitted data streams from node i can be received by all the receive nodes in $\mathcal{R}_i$ simultaneously. But the distances from node i to different nodes in $\mathcal{R}_i$ are likely to be different. As a result, the received signal strengths at different nodes in $\mathcal{R}_i$ are different, leading to different achievable data rates. So the achievable data rate is limited by the receive node in $\mathcal{R}_i$ that has the smallest SINR. Denote $c_i^k(t)$ as the achievable data rate of transmit node i's kth outgoing data stream in a one-hop multicast. Then we have

$$c_i^k(t) = \min_{j \in \mathcal{R}_i} \left\{ W \cdot \log_2 \left(1 + \frac{G_{ij} \cdot p_i^k(t)}{\sum_{h \in \mathcal{N} \setminus \mathcal{P}_j}^{h \ne i} G_{hj} \cdot P_{\rm s} \cdot x_h(t) + P_{\rm n}} \right) \right\}, \quad 1 \le i \le N, 1 \le k \le z_i(t), 1 \le t \le T, \tag{10}$$

where W is the channel bandwidth, G_{ij} is the gain of the channel between transmit node i and receive node j, and $P_{\rm n}$ is the noise power at the receiver. It should be noted that when calculating the effective SINR at receive node j in (10), we only need to consider the weak interference from the unintended transmitters in $\mathcal{N} \setminus \mathcal{P}_j$, because the strong interference from the unintended transmitters in $\mathcal{P}_j$ has been nullified in the spatial domain by IA and IC.

[4]Although there is significant research advance on full duplex in recent year, practical design of full duplex for MIMO is still in its infant stage. If we want to formulate the problem in a full-duplex network, we can simply remove (6) and (8) in this optimization framework.

Denote $c_i(t)$ as the aggregate achievable data rate at transmit node i over its $z_i(t)$ outgoing data streams in time slot t. Then we have

$$c_i(t) = \sum_{k=1}^{z_i(t)} c_i^k(t), \quad 1 \le i \le N, 1 \le t \le T\,. \tag{11}$$

Multicast Data Rate Constraints. For each multicast session, its source node wants to send data to all its destination nodes with the help from intermediate nodes. Multicast data rate refers to the end-to-end data rate from its source node to all its destination nodes. Consider the multicast tree of a session f. It has a root node, a set of internal nodes, and a set of leaves. The root node is the source node of the session and each leaf is a destination node of the session. However, an internal node can either be an intermediate node that helps relay traffic or a destination node of the session. Based on previous discussion of one-hop multicast rate constraints (9)–(11), the data rate from a node $i \in \mathcal{N}$ will be received by all of its next-hop nodes in $\mathcal{R}_i$. Therefore, for a single multicast tree f, in order to achieve its average end-to-end data rate of $r(f)$, its root node and each of its internal nodes should be able to accommodate an average rate of $r(f)$ over T time slots.

When there are multiple multicast sessions in the network (see, e.g., Fig. 2(a)), a node $i \in \mathcal{N}$ may be a root node, an internal node, or a leaf node on multiple trees. Only the first two cases (root node and internal node) are included in our discussions here. Denote $\mathcal{F}_i$ as the set of trees for which node i is used either as a root or an internal node. Then the aggregate data rate that node i needs to send out over T time slots is $\sum_{f \in \mathcal{F}_i} r(f)$. Since $\sum_{f \in \mathcal{F}_i} r(f)$ is upper bounded by the average achievable (outgoing) rate at node i, we have:

$$\sum_{f \in \mathcal{F}_i} r(f) \le \frac{1}{T} \sum_{t=1}^{T} c_i(t), \quad 1 \le i \le N\,. \tag{12}$$

Finally, since $r_{\min}$ is the minimum achievable data rate among all the multicast trees, we have:

$$r(f) \ge r_{\min}, \quad 1 \le f \le F\,. \tag{13}$$

In summary, we have the following problem formulation for multicast throughput maximization (MTM):

MTM$_1$	max	$r_{\min}$
	s.t.	Multicast IA constraints: (3)–(5);
		Multicast node constraints: (6)–(8);
		One-hop multicast rate constraints: (9)–(11);
		Multicast data rate constraints: (12)–(13);

where N, T, F, B, W, A, $P_{\rm n}$, $P_{\rm s}$, and G_{ij} are constants; $x_i(t)$ and $y_i(t)$ are binary optimization variables; $z_i(t)$ and $\alpha_{ij}(t)$ are nonnegative integer optimization variables; $r(f)$, $c_i(t)$, $p_i^k(t)$, and $c_i^k(t)$ are continuous optimization variables. In the formulation, (3)–(5) are constraints across PHY and link layers. Specifically, (3) and (4) correspond to IA and (5) corresponds to SM and IC as well as link scheduling. (6)–(8) are link-layer constraints, which correspond to link scheduling.

This article has been accepted for publication in a future issue of this journal, but has not been fully edited. Content may change prior to final publication. Citation information: DOI 10.1109/TVT.2018.2817365, IEEE Transactions on Vehicular Technology

(9)–(11) are constraints across PHY and link layers. They correspond to power allocation and link scheduling. (12)–(13) are constraints across network and transport layers. In particular, (12) corresponds to multi-hop data transmission.

This optimization problem is in the form of mixed integer nonlinear program (MINLP), which is notoriously hard to solve due to its involvement of nonlinear constraints. To reduce the complexity in the pursuit of a near-optimal solution, we show how to eliminate the nonlinear constraints in problem MTM_1 through reformulation and approximation in the next section.

V. Problem Reformulation and Approximation

In problem MTM_1, (3)–(5), (6)–(8), and (12)–(13) are linear constraints. But (9)–(11) are nonlinear constraints. The goal of this section is to perform reformulation and approximation so that the optimization problem does not contain any nonlinear constraints and is within $(1-\varepsilon)$-approximation of the original problem (MTM_1).

A. Problem Reformulation

In (9), (10), and (11), $z_i(t)$ is not a constant but rather an optimization variable. This prevents all three constraints from being linear. In addition to variable $z_i(t)$, constraint (10) also has a nonlinear function.

To linearize these constraints at transmit node i, we first reformulate $z_i(t)$ in (9), (10), and (11). To do so, we introduce $A - z_i(t)$ dummy outgoing data streams at transmit node i and add constraints to force the data rate of each dummy stream to zero. To distinguish a dummy stream from a real data stream, we define a new binary variable $\lambda_i^k(t)$ to indicate whether or not data stream k is dummy at node i in time slot t. Specifically, $\lambda_i^k(t) = 0$ if data stream k is dummy and 1 otherwise. Therefore, we have

$$\sum_{k=1}^{A} \lambda_i^k(t) = z_i(t), \quad 1 \le i \le N, 1 \le t \le T. \tag{14}$$

Consider the kth outgoing data stream at transmit node i. If $\lambda_i^k(t) = 0$ (i.e., the kth stream is dummy), then the transmit power allocated for this stream should be 0. Otherwise (i.e., $\lambda_i^k(t) = 1$), the transmit power allocated for this data stream is upper bounded by the total transmit power P_{s}. Therefore, we have

$$0 \le p_i^k(t) \le P_{\text{s}} \cdot \lambda_i^k(t), \ 1 \le i \le N, 1 \le k \le A, 1 \le t \le T. \tag{15}$$

Similarly, we use the following constraints to force the achievable data rate of a dummy data stream to zero:

$$0 \le c_i^k(t) \le B \cdot \lambda_i^k(t), \quad 1 \le i \le N, 1 \le k \le A, 1 \le t \le T, \tag{16}$$

where B is a sufficiently large constant number that we defined earlier.

New constraints (14)–(16) ensure that a dummy data stream has zero transmit power and zero data rate. With the notion of dummy stream and constraints (14)–(16), constraint (9) can be rewritten as:

$$\sum_{k=1}^{A} p_i^k(t) = P_{\text{s}} \cdot x_i(t), \quad 1 \le i \le N, 1 \le t \le T. \tag{17}$$

Constraint (11) can be rewritten as:

$$c_i(t) = \sum_{k=1}^{A} c_i^k(t), \quad 1 \le i \le N, 1 \le t \le T. \tag{18}$$

Constraint (10) can be rewritten as:

$$c_i^k(t) = \min_{j \in \mathcal{R}_i} \left\{ W \cdot \log_2 \Big(1 + \frac{G_{ij} \cdot p_i^k(t)}{\sum_{h \in \mathcal{N} \setminus \mathcal{P}_j}^{h \neq i} G_{hj} \cdot P_{\text{s}} \cdot x_h(t) + P_{\text{n}}} \Big) \right\}, \quad 1 \le i \le N, 1 \le k \le A, 1 \le t \le T. \tag{19}$$

Since constraints (14)–(18) are linear, we now focus on the only nonlinear constraint (19), which contains a fraction and a log function. In what follows, we first linearize the fraction and then address the log function in Section V-B.

Denote $\gamma_{ij}^k(t)$ as:

$$\gamma_{ij}^k(t) = \frac{G_{ij} \cdot p_i^k(t)}{\sum_{h \in \mathcal{N} \setminus \mathcal{P}_j}^{h \neq i} G_{hj} \cdot P_{\text{s}} \cdot x_h(t) + P_{\text{n}}}, \quad 1 \le i \le N, j \in \mathcal{R}_i, 1 \le k \le A, 1 \le t \le T. \tag{20}$$

Then (20) can be equivalently rewritten as:

$$\sum_{h \in \mathcal{N} \setminus \mathcal{P}_j}^{h \neq i} G_{hj} \cdot P_{\text{s}} \cdot x_h(t) \cdot \gamma_{ij}^k(t) + P_{\text{n}} \cdot \gamma_{ij}^k(t) = G_{ij} \cdot p_i^k(t), \quad 1 \le i \le N, j \in \mathcal{R}_i, 1 \le k \le A, 1 \le t \le T. \tag{21}$$

Constraint (21) is still nonlinear since it has nonlinear term $x_h(t) \cdot \gamma_{ij}^k(t)$. To handle the product of variables, we employ the Reformulation-Linearization Technique (RLT) [26, Chapter 6]. Define a new variable $w_{ij}^{hk}(t) = x_h(t) \cdot \gamma_{ij}^k(t)$. Then (21) can be rewritten as:

$$\sum_{h \in \mathcal{N} \setminus \mathcal{P}_j}^{h \neq i} G_{hj} \cdot P_{\text{s}} \cdot w_{ij}^{hk}(t) + P_{\text{n}} \cdot \gamma_{ij}^k(t) = G_{ij} \cdot p_i^k(t), \quad 1 \le i \le N, j \in \mathcal{R}_i, 1 \le k \le A, 1 \le t \le T. \tag{22}$$

To ensure that $w_{ij}^{hk}(t) = x_h(t) \cdot \gamma_{ij}^k(t)$ holds, we add the following two sets of linear constraints to our new formulation:

$$0 \le w_{ij}^{hk}(t) \le \gamma_{ij}^k(t), \quad 1 \le i \le N, j \in \mathcal{R}_i, 1 \le k \le A, h \in \mathcal{N} \setminus \mathcal{P}_j \setminus \{i\}, 1 \le t \le T. \tag{23}$$

$$\gamma_{ij}^k(t) - [1 - x_h(t)] \cdot B \le w_{ij}^{hk}(t) \le x_h(t) \cdot B, \quad 1 \le i \le N, j \in \mathcal{R}_i, 1 \le k \le A, h \in \mathcal{N} \setminus \mathcal{P}_j \setminus \{i\}, 1 \le t \le T, \tag{24}$$

where B is a sufficiently large number that we defined earlier. Now (21) can be replaced with constraints (22)–(24). Based on the definition of $\gamma_{ij}^k(t)$, nonlinear constraint (19) can be rewritten as:

$$c_i^k(t) = \min_{j \in \mathcal{R}_i} \left\{ W \cdot \log_2 \left(1 + \gamma_{ij}^k(t) \right) \right\}, \quad \begin{array}{l} 1 \le i \le N, 1 \le k \le A, \\ 1 \le t \le T, \end{array}$$

which is equivalent to:

$$c_i^k(t) \le W \cdot \log_2 \left(1 + \gamma_{ij}^k(t) \right), \quad \begin{array}{l} 1 \le i \le N, j \in \mathcal{R}_i, \\ 1 \le k \le A, 1 \le t \le T. \end{array} \tag{25}$$

By replacing (9)–(11) with (14)–(18) and (22)–(25), problem MTM_1 is reformulated as:

This article has been accepted for publication in a future issue of this journal, but has not been fully edited. Content may change prior to final publication. Citation information: DOI 10.1109/TVT.2018.2817365, IEEE Transactions on Vehicular Technology

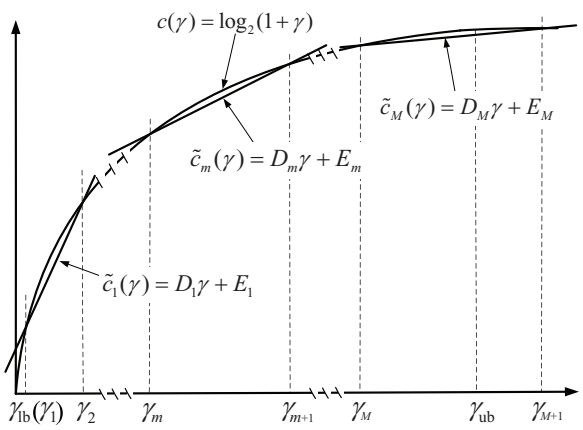

Fig. 5: A linear approximation for log function $c_1(\gamma) = \log_2(1+\gamma)$.

Algorithm 1 Computing D_m, E_m, and M.

// Initialization
$\gamma_{\rm lb} = \max_{i,j\in\mathcal{N}}\{G_{ij}P_{\rm s}/P_{\rm n}\}$;
$\gamma_{\rm ub} = \min_{i,j\in\mathcal{N}}\{G_{ij}P_{\rm s}/(\sum_{k\in\mathcal{N}}^{k\neq i,j} G_{kj}P_{\rm s}+P_{\rm n})\}$;
$m = 0$;
$\gamma_1 = \gamma_{\rm lb}$;
// Main loop
while $\gamma_m < \gamma_{\rm ub}$ **do**
  $m \leftarrow m+1$;
  $\gamma_{m+1} = b_{m,1} + \sqrt{b_{m,1}^2 - 4b_{m,2}} - \gamma_m$ where
  $b_{m,1} = 2\gamma_m + \varepsilon(1+\gamma_m)\ln(1+\gamma_m)$ and
  $b_{m,2} = \gamma_m^2 - \varepsilon(1+\gamma_m)\ln(1+\gamma_m)$;
  $D_m = \frac{\log_2(1+\gamma_{m+1})-\log_2(1+\gamma_m)}{\gamma_{m+1}-\gamma_m}$;
  $E_m = \log_2(1+\gamma_m) - \frac{\gamma_m[\log_2(1+\gamma_{m+1})-\log_2(1+\gamma_m)]}{\gamma_{m+1}-\gamma_m}$;
end while
$M = m$;

MTM$_2$ max $r_{\min}$
s.t. Multicast IA constraints: (3)–(5);
Multicast node constraints: (6)–(8);
Multicast data rate constraints: (12)–(13);
One-hop multicast rate constraints: (14)–(18), (22)–(25).

Denote $r^*_{\min}(\mathrm{MTM}_1)$ and $r^*_{\min}(\mathrm{MTM}_2)$ as the optimal objective values of MTM$_1$ and MTM$_2$, respectively. We have the following lemma:

Lemma 2: Problems MTM$_1$ and MTM$_2$ have the same optimal objective value, i.e., $r^*_{\min}(\mathrm{MTM}_1) = r^*_{\min}(\mathrm{MTM}_2)$.

Lemma 2 can be proved by construction. Specifically, for an optimal solution to problem MTM$_1$, we can always construct a feasible solution to problem MTM$_2$ that achieves the optimal objective value of MTM$_1$, and vice versa. As the proof is straightforward, we omit it to save space.

B. $(1-\varepsilon)$-Optimal Approximation

In problem MTM$_2$, all constraints are linear except (25). To linearize the log function in (25), we resort to linear approximation. The goal is to replace the log function with a minimum number of linear constraints while ensuring the gap between the two never exceeds ε, a target performance gap for the objective value.

In (25), γ_{ij}^k is the signal to interference plus noise ratio (SINR) of a data stream from transmit node i to its intended receive node j (see (20)). To linearize the log function, we first characterize the range of its variable γ_{ij}^k. Note that the range for each link may differ due to difference of link distance. So, instead of finding the range for each individual link (i,j), we use a universal lower bound $\gamma_{\rm lb}$ and a universal upper bound $\gamma_{\rm ub}$ for all links. The range of γ_{ij}^k for each link (i,j) will fall in $[\gamma_{\rm lb},\ \gamma_{\rm ub}]$. Therefore, instead of designing a unique linear approximation (for the log function) for each individual link (i,j), we will use one (identical) linear approximation for the log function, over the range of $[\gamma_{\rm lb},\ \gamma_{\rm ub}]$, for all links. Note that, as we will prove in Theorem 2, the use of an identical linear approximation for all links will not induce any infeasible solution. For an upper bound $\gamma_{\rm ub}$, we can use the best possible scenario where there is no interference at receive node j, i.e., $\gamma_{\rm ub} = \max_{i,j\in\mathcal{N}}\{G_{ij}P_{\rm s}/P_{\rm n}\}$. For a lower bound $\gamma_{\rm lb}$, we can use the worst-case scenario where all other nodes in the network are transmitters and interfering with receive node j, i.e., $\gamma_{\rm lb} = \min_{i,j\in\mathcal{N}}\left\{G_{ij}P_{\rm s}/(\sum_{k\in\mathcal{N}}^{k\neq i,j} G_{kj}P_{\rm s}+P_{\rm n})\right\}$.

As illustrated in Fig. 5, to approximate the log function $c(\gamma) = \log_2(1+\gamma)$ over $[\gamma_{\rm lb},\ \gamma_{\rm ub}]$, we need multiple lines. Denote the set of lines as $\left\{\tilde{c}_m(\gamma) = D_m\cdot\gamma + E_m : 1 \le m \le M\right\}$, where m is the line sequence number, D_m is the slope, and E_m is the vertical starting point of the line. M is the minimum number of required lines for the approximation, which will be calculated later. To start with, let's consider the first line $\tilde{c}_1(\gamma) = D_1\cdot\gamma + E_1$. Denote γ_1 and γ_2 as the two points on $\log_2(1+\gamma)$ where the line intersects (see Fig. 5). Then $\gamma_1 = \gamma_{\rm lb}$. For γ_2, we shall find the maximum value so that the performance gap of this line approximation is upper bounded by ε, i.e.,

$$0 \le \frac{c(\gamma)-\tilde{c}_1(\gamma)}{c(\gamma)} \le \varepsilon, \quad \forall\gamma\in[\gamma_1,\ \gamma_2]\,. \tag{26}$$

Through some algebraic manipulations, we find that

$$\gamma_2 = b_1 + \sqrt{b_1^2 - 4b_2} - \gamma_1\ ,$$

where $b_1 = 2\gamma_1 + \varepsilon(1+\gamma_1)\ln(1+\gamma_1)$ and $b_2 = \gamma_1^2 - \varepsilon(1+\gamma_1)\ln(1+\gamma_1)$. Then we can find D_1 and E_1 in $\tilde{c}_1(\gamma) = D_1\cdot\gamma + E_1$ as:

$$D_1 = \frac{\log_2(1+\gamma_2)-\log_2(1+\gamma_1)}{\gamma_2-\gamma_1}\ ,$$
$$E_1 = \log_2(1+\gamma_1) - D_1\cdot\gamma_1\ .$$

After obtaining the first line, we can compute the second by following the same token, but starting from point $(\gamma_2, \log_2(1+\gamma_2)$. Subsequently, we can compute all the lines over range $[\gamma_{\rm lb},\ \gamma_{\rm ub}]$. The procedure of computing the parameters of the approximation lines is given in Alg. 1. Note that our procedure yields the minimum number of lines to approximate the log function.

This article has been accepted for publication in a future issue of this journal, but has not been fully edited. Content may change prior to final publication. Citation information: DOI 10.1109/TVT.2018.2817365, IEEE Transactions on Vehicular Technology

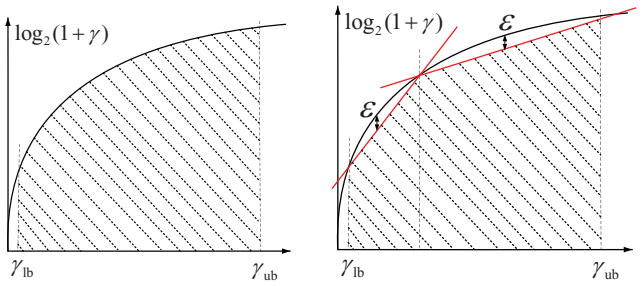

(a) Original feasible region. (b) Approximated feasible region.

Fig. 6: Original and approximated feasible regions.

We now employ Alg. 1 to linearize the log function in (25) in MTM_2. For (25), its feasible region is within the shadowed area beneath the log curve as shown in Fig. 6(a). We approximate this area by a polygon defined by the lines generated in Alg. 1 over $[\gamma_{lb}, \gamma_{ub}]$ as shown in Fig. 6(b). Therefore, (25) can be approximated by the following constraint:

$$c_i^k(t) \le W \cdot \big(D_m \gamma_{ij}^k(t) + E_m\big), \quad \begin{array}{l} 1 \le i \le N, j \in \mathcal{R}_i, 1 \le k \le A, \\ 1 \le t \le T, 1 \le m \le M \end{array}, \tag{27}$$

where M, D_m, and E_m are computed in Alg. 1.

By replacing (25) in MTM_2 with (27), the resulting optimization problem, which we denote as MTM_3, can be written as:

$\textbf{MTM}_3$ max $r_{\min}$
s.t. Multicast IA constraints: (3)–(5);
Multicast node constraints: (6)–(8);
Multicast data rate constraints: (12)–(13);
One-hop multicast rate constraints: (14)–(18), (22)–(24), (27).

Denote $r_{\min}^*(\text{MTM}_3)$ as the optimal objective value of MTM_3. Then we have the following theorem:

Theorem 2: The optimal objective value of MTM_3 is a $(1-\varepsilon)$ approximation of the optimal objective value of MTM_2, i.e., $(1-\varepsilon) \cdot r_{\min}^*(\text{MTM}_2) \le r_{\min}^*(\text{MTM}_3) \le r_{\min}^*(\text{MTM}_2)$.

The proof of Theorem 2 is given in Appendix C. Combining Theorem 2 and Lemma 2, we have the following corollary:

Corollary 1: The optimal objective value of MTM_3 is a $(1-\varepsilon)$ approximation of the optimal objective value of MTM_1, i.e., $(1-\varepsilon) \cdot r_{\min}^*(\text{MTM}_1) \le r_{\min}^*(\text{MTM}_3) \le r_{\min}^*(\text{MTM}_1)$.

This corollary is straightforward and we omit its proof to conserve space.

In summary, we have successfully transformed MTM_1 (a MINLP) to MTM_3, which is a mixed integer linear program (MILP). Although the theoretical worst-case complexity of solving a general MILP problem is exponential, there exist highly efficient optimal algorithms (e.g., branch-and-bound with cutting planes [27]) and heuristic algorithms (e.g., sequential fixing algorithm [26, Chapter 10]). For most of practical-sized networks, an off-the-shelf optimization solver such as IBM CPLEX [28] is also very effective. Since the goal of this paper is to explore the throughput gain of multicast IA in a multi-hop MIMO network, we will employ optimization solver IBM CPLEX in our performance evaluation.

C. Discussions

Some discussions of the multicast IA model and the throughput maximization problem are presented as follows.

Optimality of Multicast IA Model: For the multicast IA scheme in Section III-B, we proved its feasibility but did not provide any analysis on its optimality (i.e., tightness of the feasibility constraints). As our IA scheme imposed a special structure at the receiver side (to analytically prove its feasibility), the resulting IA solution is an approximation to the optimal solution. How to design an optimal multicast IA scheme that can fully utilize the freedom in the transceiver design remains open [30] and beyond the scope of this paper.

Fixed Interference Range: In our problem formulation, we employed a fixed interference range to classify strong and weak interferences. The classification method is simple but does not take into account small-scale channel fading effect, and therefore is not accurate. However, we want to point out that our multicast IA model and optimization formulation can easily adopt the strength-based interference classification method, as the set of interfering transmitters for each receiver is not a part of optimization problem but a part of network setting.

Practical Implementation: This paper serves as a pioneer exploration on IA for multicast communications in multi-hop MIMO networks. It outlined a multicast IA scheme and derived its feasible region by defining a set of simple constraints. To employ this multicast IA scheme in practical systems, there are many technical details that need to be addressed, such as node coordination, CSI acquisition, transmission synchronization, and management of error propagation. These issues are not the main focus of this paper and we plan to address them in our future work.

VI. Performance Evaluation

In this section, we conduct performance evaluation of IA for multicast communications in multi-hop MIMO networks. We will use IBM CPLEX [28] to solve problem MTM_3 and compare its optimal objective value against that when IA is not used.

A. Simulation Setting

We consider a multi-hop MIMO network with 30 nodes randomly deployed in a 1000m $\times$ 1000m square area. For each node in the network, we assume that it has a transmit power of 23 dBm when transmitting as this is the typical maximum transmit power for many wireless devices. To compute the path loss from a transmitter to a receiver, we adopt the formula in LTE specification (3GPP TR 25.951 V10.0.0). Specifically, the power attenuation from node i to node j is calculated by $G_{ij} = 10^{-L_{\text{PL}}/10}$ with $L_{\text{PL}} = 32.9 + 37.5 \log_{10}(d_{ij})$, where d_{ij} is the distance between them. The channel bandwidth is 10 MHz, which is a typical bandwidth in many broadband wireless systems such as Wi-Fi and LTE. Empirically, we assume the noise power at a receive node to be -104 dBm and the transmission range of a node to be 300 m. We will discuss interference range later.

This article has been accepted for publication in a future issue of this journal, but has not been fully edited. Content may change prior to final publication. Citation information: DOI 10.1109/TVT.2018.2817365, IEEE Transactions on Vehicular Technology

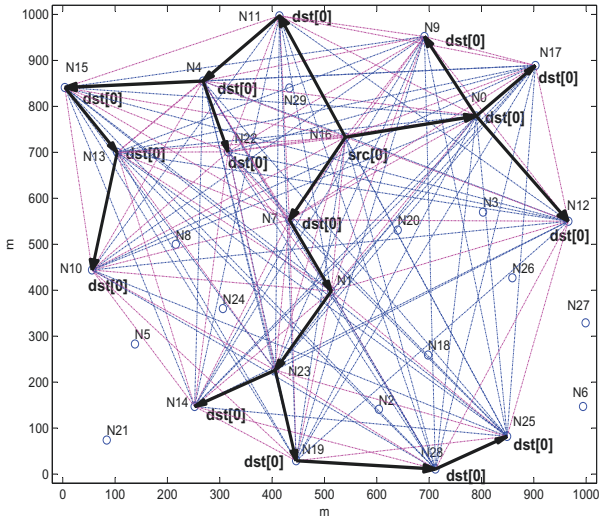

Fig. 7: A network instance for case study.

For each multicast session, its source and destination nodes are randomly selected among all the nodes in the network. The transmission scheduling is based on time slots and there are four time slots in a frame. The routing tree for the multicast session is computed by the OSPF protocol [25]. To tolerate 5% performance loss, we set the approximation error ε to 5%.

B. Impact of Interference Range Φ

In Section III-B, we use interference range Φ to classify an interference as either a strong or a weak interference at a receiver. The strong interferences will be handled by MIMO's IA and IC, while the weak interferences will be treated as noise. Therefore, the setting of Φ is important in solving problem MTM_3.

To see the impact of Φ on the objective value of MTM_3, consider an example network instance shown in Fig. 7, where each node has four antennas (i.e., $A = 4$). In this network, we have one multicast session with one source node (denoted as src$[0]$ in the figure) and 15 destination nodes (denoted as dst$[0]$ in the figure). The multicast routing tree in Fig. 7 was found by OSPF [25]. In Fig. 8(a), we present the normalized throughput w.r.t. bandwidth (in bit/s/Hz) under different settings of Φ. The normalized throughput is obtained by solving the problem MTM_3 using CPLEX. In Fig. 8(a), $\Phi = 0$ represents the special case where all interferences are treated as noise at each receiver. In this case, neither IA nor IC will be used. Without IA and IC, those strong interferences will be treated as noise in the SINR calculation at each receiver, which will severely reduce the achievable throughput. Not surprisingly, this point ($\Phi = 0$) represents the smallest throughput for all settings of Φ.

When $\Phi > 0$, the normalized throughput varies and depends on the setting of Φ:

- When $0 \leq \Phi \leq 600$, the normalized throughput is strictly increasing with the value of Φ. This is because the increase of Φ allows more strong interferences to be nullified through MIMO's IA and IC. As a result, the SINR at each receiver increases, so does the achievable rate of a session.
- When $600 \leq \Phi \leq 1414$, the normalized throughput decreases with Φ. This is because increase of Φ results in the use of MIMO's DoFs to cancel weak interferences, leaving fewer DoFs available for data transmission.
- When $\Phi \geq 1414$, the normalized throughput flattens out. Since 1414 is the farthest possible distance between any two nodes in a 1000×1000 area, all the interferences at a receiver are considered as strong interference and handled by IA and IC. Further increase of Φ will no longer affect the classification of strong or weak interference in the network. Therefore, the normalized throughput will stay flat.

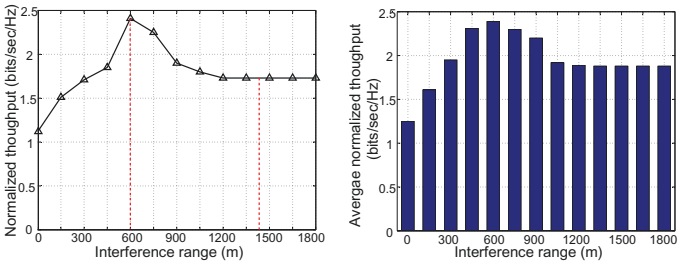

(a) One network instance (b) 100 network instances

Fig. 8: Impact of Φ on normalized throughput.

In Fig. 8(b), we present the average throughput (normalized w.r.t. bandwidth) over 100 network instances under different settings of Φ. The results are in agreement with our findings in Fig. 8(a). Note that, for this network setting, the peak throughput occurs when the interference range ($\Phi = 600$) is twice the transmission range (300). This is not surprising, and is consistent with the findings by Shi et al. in [29].

C. Throughput Performance

For the rest of this section, we set $\Phi = 600$. We will compare the multicast throughput of a network with IA (obtained by solving MTM_3) against the throughput of the same network without IA. The formulation of the latter problem, denoted as MTM-noIA, is given in Appendix D.

Impact of Antenna Number. We first study throughput under different antenna configurations (i.e., the number of antennas at each node). We consider 100 randomly generated 30-node network instances, each of which has one multicast session with one source node and 15 destination nodes. For each network instance, the source and destination nodes are randomly selected. Fig. 9(a) presents the average multicast throughput of the 100 network instances under different antenna configurations. Fig. 9(b) presents the corresponding multicast throughput gain of IA under different antenna configurations. For example, when each node has 5 antennas, the average multicast throughput of the 100 network instances is 2.06 (without IA) and 2.89 (with IA), as shown in Fig. 9(a). Therefore, the throughput gain is $(2.89 - 2.06)/2.06 \approx 40\%$, as shown in Fig. 9(b).

Fig. 9 shows that the multicast throughput increases with the number of antennas. Furthermore, the throughput gain of

This article has been accepted for publication in a future issue of this journal, but has not been fully edited. Content may change prior to final publication. Citation information: DOI 10.1109/TVT.2018.2817365, IEEE Transactions on Vehicular Technology

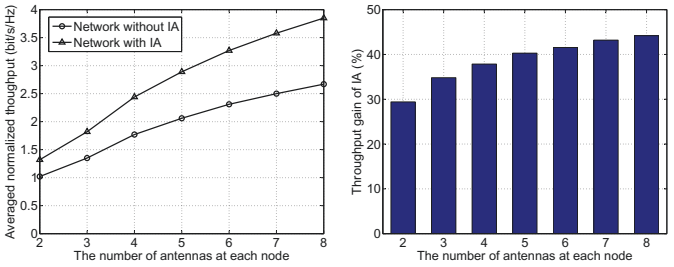

(a) Averaged throughput comparison under different number of antennas

(b) Averaged throughput gain under different number of antennas

Fig. 9: Impact of antenna number on normalized average throughput.

TABLE II: Average multicast throughput (normalized w.r.t. bandwidth) over 100 network instances.

(a) Normalized throughput under different multicast group sizes

Multicast group size	1	5	10	15	20	25	29
Throughput without IA	6.28	2.81	2.06	1.78	1.50	1.33	1.23
Throughput with IA	6.53	3.30	2.71	2.39	2.07	1.85	1.72

(b) Normalized throughput under different multicast session numbers

# of multicast sessions	1	2	3	4	5	6	7
Throughput without IA	3.56	1.80	1.07	0.72	0.55	0.41	0.28
Throughput with IA	3.88	2.30	1.49	1.04	0.82	0.62	0.43

IA becomes more significant when the number of antennas increases. This is because more antennas provide more spatial DoFs to perform IA, thus offering a higher throughput gain of IA. Since the throughput gain of IA increases with the number of antennas on each node, an ideal application scenario of our proposed IA solution is massive MIMO networks where each node has a large number of antennas.

Impact of Multicast Group Size. We now study the impact of multicast group size (i.e., the number of destination nodes in a multicast session) on network throughput. We consider 100 randomly generated 30-node network instances, where each node has four antennas. Each network instance has one multicast session and its destination group size varies from 1 (unicast), 5, 10, $\cdots$, to 29 (broadcast). Table II(a) presents the average multicast throughput (over 100 network instances) for different group sizes. Figure 10(a) presents the corresponding multicast throughput gain of IA under different multicast group sizes. For example, when the multicast group size is 15, the average multicast throughput of the 100 network instances is 1.78 (without IA) and 2.39 (with IA), as shown in Table II(a). Therefore, the percentage of multicast throughput gain by IA is $(2.39 - 1.78)/1.78 \approx 34\%$, as shown in Fig. 10(a).

From Table II(a) and Fig. 10(a), we can see that, although the multicast throughput decreases as the multicast group size increases (see Table II(a)), the throughput gain of IA becomes more significant as the multicast group size increases (see Fig. 10(a)). This can be explained by the fact that a larger

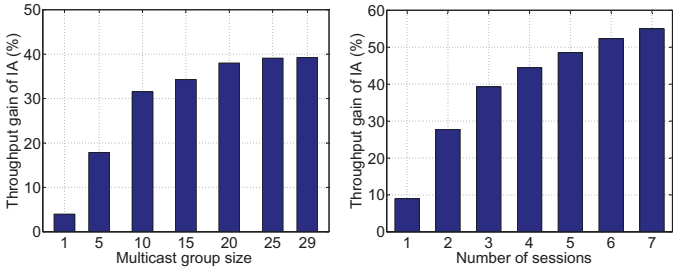

(a) Throughput gain under different multicast group sizes

(b) Throughput gain under different session numbers

Fig. 10: Multicast throughput performance of IA.

multicast group size leads to more interference in the network and therefore offers more opportunities for IA.

Impact of Session Number. We now study throughput when the number of multicast session increases. Again we consider 100 randomly generated 30-node network instances and each node has four antennas. For each network instance, we vary the number of multicast sessions. For each multicast session, it has three destination nodes, again chosen randomly. Table II(b) presents the average multicast throughput (over 100 network instances) when the networks have different numbers of multicast sessions. Figure 10(b) presents the corresponding multicast throughput gain of IA. For example, when the number of sessions is 4, the average multicast throughput is 0.72 (without IA) and 1.04 (with IA), as shown in Table II(b). Then the percentage of multicast throughput gain by IA is $(1.04 - 0.72)/0.72 \approx 44\%$, as shown in Fig. 10(b).

From Table II(b) we can see that the multicast throughput of a network (with or without IA) decreases as the number of sessions increases. If we keep increasing the number of sessions in the network, the throughput (the optimal objective value of MTM_3) will eventually go to 0. This is because if there are too many links on the multicast trees, some of them cannot be active due to limited resources (MIMO's DoFs and time slots). But within the schedulable region (nonzero throughput region) of the network, we can see from Fig. 10(b) that the multicast throughput gain of IA becomes more significant as the number of multicast sessions increases. This is intuitive, as the more multicast sessions in the network, the more interference among the links, thereby offering more opportunities for IA among the interferences.

VII. Conclusions

The potential of IA is most profound when there are enough opportunities to align interfering signals at a receiver. Multicast communications offer a natural environment to exploit IA's potential. In this paper, we offer a systematic study of IA for multicast communications in a multi-hop MIMO network. Instead of dealing with complex design of precoding and decoding vectors, we developed a set of linear constraints at both transmitter and receiver to characterize a feasible design space for multicast IA. We showed that, for a set of data streams, as long as the set of linear constraints are satisfied, there exist feasible precoding and decoding vectors at the PHY layer. The set of proposed constraints renders a simple mathematical abstraction to study multicast IA without being

This article has been accepted for publication in a future issue of this journal, but has not been fully edited. Content may change prior to final publication. Citation information: DOI 10.1109/TVT.2018.2817365, IEEE Transactions on Vehicular Technology

buried by the onerous signal design at the PHY layer. Based on these constraints, we formulated a multicast throughput maximization problem and employed $(1-\varepsilon)$-approximation techniques to linearize the nonlinear constraints. Simulation results showed significant throughput gain of IA for multicast communications. Within the schedulable region (with non-zero throughput), we find that the throughput gain of IA increases with the number of antennas, the size of multicast group, and the number of multicast sessions.

APPENDIX A
PROOF OF LEMMA 1

We show that the interfering streams from transmit node i can be aligned successfully at receive node k by construction. For the interfering streams from other transmit nodes in $\mathcal{P}_k$ (e.g., h and l in Fig. 4), they can be successfully aligned in the same way as transmit node i.

At receive node k, denote $\mathcal{Z}_i$ as the set of its interfering streams from transmit node i. Among the interfering streams in $\mathcal{Z}_i$, denote $\mathcal{A}_{ik}$ as the subset of interfering streams that should be aligned (to other interfering streams) at receive node k. By definition, we have $|\mathcal{Z}_i| = z_i(t)$ and $|\mathcal{A}_{ik}| = \alpha_{ik}(t)$. To align the interfering streams in $\mathcal{A}_{ik}$ at receive node k, we employ the following IA scheme: for each interfering stream in $\mathcal{A}_{ik}$, we align it to a *unique* interfering stream in $\cup_{h\in\mathcal{P}_k}^{h\neq i}\mathcal{Z}_h\backslash\mathcal{A}_{hk}$. By "unique" we mean that any two interfering streams in $\mathcal{A}_{ik}$ are not allowed to align to the same (a third) interfering stream at receive node k. Based on the given constraint (4), we know that the number of interfering streams in $\cup_{h\in\mathcal{P}_k}^{h\neq i}\mathcal{Z}_h\backslash\mathcal{A}_{hk}$ is more than that in $\mathcal{A}_{ik}$. So every interfering stream in $\mathcal{A}_{kj}$ can be successfully aligned in this IA scheme. For this IA scheme, it is not difficult to see that it meets the requirement (i.e., any two interfering streams from transmit node $i \in \mathcal{P}_k$ are not to be aligned to the same direction at receive node k). Therefore, this lemma holds.

APPENDIX B
PROOF OF THEOREM 1

As IA in each time slot is independent, it suffices to prove Theorem 1 for any one time slot. Consider the network in time slot $t \in [1, T]$. Denote N_{T} as the number of transmitters and index the transmitters from 1 to N_{T}. Denote N_{R} as the number of receivers and index the receivers from 1 to N_{R}. Further, without loss of generality, we omit time slot index t in (3), (4), and (5). Then, for constraint (3), it can be written as:

$$\sum_{j\in\mathcal{Q}_i}\alpha_{ij} \le z_i, \quad 1 \le i \le N_{\mathrm{T}}. \tag{28}$$

For constraint (4), it can be written as:

$$\alpha_{ij} \le \sum_{h\in\mathcal{P}_j}^{h\neq i}[z_h - \alpha_{hj}], \quad 1 \le j \le N_{\mathrm{R}}, i \in \mathcal{P}_j. \tag{29}$$

For constraint (4), when $y_j = 0$ (i.e., node j is not a receiver), this constraint is not effective as B is a sufficiently large number; when $y_j = 1$ (i.e., node j is a receiver), (4) can be equivalently written as:

$$\sum_{i\in\mathcal{T}_j} z_i + \sum_{i\in\mathcal{P}_j}[z_i - \alpha_{ij}] \le A, \quad 1 \le j \le N_{\mathrm{R}}. \tag{30}$$

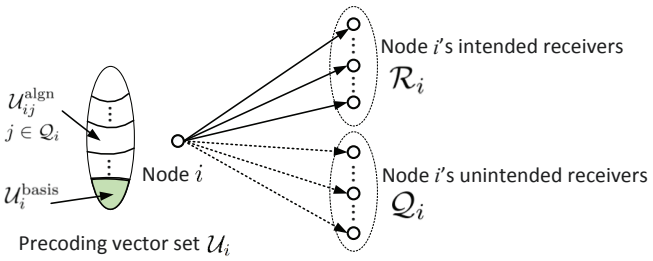

Fig. 11: At a transmitter: signal, interference, and precoding vectors.

Recall that $\mathbf{u}_i^k$, $1 \le k \le z_i$, is transmitter i's kth precoding vector and $\mathbf{v}_{ij}^k$, $i \in \mathcal{T}_j$, $1 \le k \le z_i$, is receiver j's decoding vector used to decode transmit i's kth data stream. We have the following definition.

Definition 1: A DoF vector $\varphi = (z_1, z_2, \cdots, z_{N_{\mathrm{T}}})$ is feasible if each transmit node i can send z_i data streams to its one-hop multicast receive nodes in R_i free of strong interference, i.e., for $1 \le i \le N_{\mathrm{T}}$, $j \in \mathcal{R}_i$, and $1 \le k \le z_i$, there exist precoding vector $\mathbf{u}_i^k$ and decoding vector $\mathbf{v}_{ij}^k$ such that

$$(\mathbf{v}_{ij}^k)^T\mathbf{H}_{ji}\mathbf{u}_i^k = 1, \tag{31a}$$

$$(\mathbf{v}_{ij}^k)^T\mathbf{H}_{ji'}\mathbf{u}_{i'}^{k'} = 0, \quad i' \in \mathcal{P}_j \cup \mathcal{T}_j, 1 \le k' \le z_{i'}. \tag{31b}$$

Simply put, to prove Theorem 1, we show that if DoF vector $\varphi = (z_1, z_2, \cdots, z_{N_{\mathrm{T}}})$ satisfies (1), (2), and (3), then we can always construct precoding and decoding vectors that meet (4a) and (4b) for $1 \le i \le N_{\mathrm{T}}$, $j \in \mathcal{R}_i$, and $1 \le k \le z_i$. It should be noted that (31a) and (31b) are bilinear equations and a general solution to a set of bilinear equations remains an open problem.

For receiver i as shown in Fig. 11, denote $\mathcal{U}_i$ as the set of precoding vectors at transmitter i, i.e., $\mathcal{U}_i = \{\mathbf{u}_i^k : 1 \le k \le z_i\}$. Then, we consider a receiver j as shown in Fig. 12. Denote $\mathcal{D}_j^{\mathrm{S}}$ as the set of *data stream* directions at receiver j. Denote $\mathcal{D}_j^{\mathrm{I}}$ as the set of *interfering stream* directions at receiver j. Mathematically, we have

$$\mathcal{D}_j^{\mathrm{S}} = \bigcup_{i\in\mathcal{T}_j}\{\mathbf{H}_{ji}\mathbf{u}_i^k : \mathbf{u}_i^k \in \mathcal{U}_i\},$$

$$\mathcal{D}_j^{\mathrm{I}} = \bigcup_{i\in\mathcal{P}_j}\{\mathbf{H}_{ji}\mathbf{u}_i^k : \mathbf{u}_i^k \in \mathcal{U}_i\}.$$

The following lemma shows a sufficient condition for DoF vector φ to be feasible.

Lemma 3: A DoF vector $\varphi = (z_1, z_2, \cdots, z_{N_{\mathrm{T}}})$ is feasible if $(z_1, z_2, \cdots, z_{N_{\mathrm{T}}})$ satisfies

$$\dim(\mathcal{D}_j^{\mathrm{S}} \cup \mathcal{D}_j^{\mathrm{I}}) = \sum_{i\in\mathcal{T}_j} z_i + \dim(\mathcal{D}_j^{\mathrm{I}}), \quad 1 \le j \le N_{\mathrm{R}}. \tag{32}$$

This article has been accepted for publication in a future issue of this journal, but has not been fully edited. Content may change prior to final publication. Citation information: DOI 10.1109/TVT.2018.2817365, IEEE Transactions on Vehicular Technology

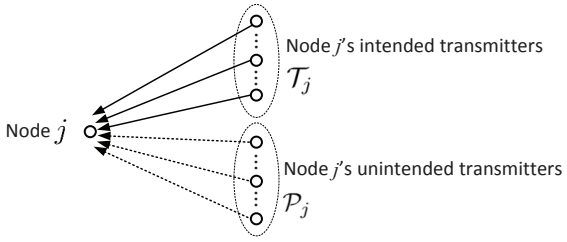

Fig. 12: At a receiver: signal and interference.

Proof. We show DoF vector φ is feasible by arguing that if (32) is satisfied, then we can always construct decoding vectors $\{\mathbf{v}_{ij}^k : i \in \mathcal{T}_j, 1 \leq k \leq z_i\}$ at receiver j such that (31a) and (31b) are satisfied. That is, we show that the following linear system is consistent if (32) is satisfied.

$$(\mathbf{v}_{ij}^k)^T \mathbf{H}_{ji} \mathbf{u}_i^k = 1, \tag{33a}$$

$$(\mathbf{v}_{ij}^k)^T \mathbf{H}_{ji'} \mathbf{u}_{i'}^{k'} = 0, \quad i' \in \mathcal{P}_j \cup \mathcal{T}_j, 1 \leq k' \leq z_{i'}. \tag{33b}$$

Based on the definition of $\mathcal{D}_j^{\mathrm{S}}$ and $\mathcal{D}_j^{\mathrm{I}}$, we know

$$\mathcal{D}_j^{\mathrm{S}} \cup \mathcal{D}_j^{\mathrm{I}} = \bigcup_{i \in \mathcal{T}_j \cup \mathcal{P}_j} \left\{ \mathbf{H}_{ji'} \mathbf{u}_{i'}^{k'} : i' \in \mathcal{U}_i \right\}.$$

It is easy to see that $\mathcal{D}_j^{\mathrm{S}} \cup \mathcal{D}_j^{\mathrm{I}}$ is the set of coefficient-vectors of this linear system. Moreover, this system has A free variables and at most A linearly independent equations. If we can show that vector $\mathbf{H}_{ji}\mathbf{u}_i^k$ is not a linear combination of other vectors in $\mathcal{D}_j^{\mathrm{S}} \cup \mathcal{D}_j^{\mathrm{I}}$, then this system is consistent. We prove this point by contradiction.

Suppose that $\mathbf{H}_{ji}\mathbf{u}_i^k$ is a linear combination of other vectors in $\mathcal{D}_j^{\mathrm{S}} \cup \mathcal{D}_j^{\mathrm{I}}$. Since $\mathbf{H}_{ji}\mathbf{u}_i^k \in \mathcal{D}_j^{\mathrm{S}}$, we have

$$\dim(\mathcal{D}_j^{\mathrm{S}} \cup \mathcal{D}_j^{\mathrm{I}}) < |\mathcal{D}_j^{\mathrm{S}}| + \dim(\mathcal{D}_j^{\mathrm{I}}) = \sum_{i \in \mathcal{T}_j} z_i + \dim(\mathcal{D}_j^{\mathrm{I}}).$$

But this contradicts (32). Thus, we conclude that the linear system is consistent. □

Intuitively, Lemma 3 says that at receiver j, if a desired data stream lies in an independent direction (i.e., not within the subspace spanned by other data/interfering streams), then this data stream is resolvable. Lemma 3 offers another way to check the feasibility of a given DoF vector: Instead of constructing both precoding and decoding vectors to satisfy (31a) and (31b) in Definition 1, it suffices to construct precoding vectors only to satisfy (32) in Lemma 3.

A. Road-Map of Our Proof

The road-map for the rest of our proof is as follows.

- *Step 1 (Precoding Vector Assignment and IA Scheme):* Based on the constraints in the IA model, we propose a precoding vector assignment scheme at each transmitter and an IA scheme at each receiver. The objective of our precoding vector assignment is to ensure that for each pair of interfering nodes (i, j), α_{ij} interfering streams can be successfully aligned to any particular directions. The objective of our IA scheme is to ensure the desired data streams at each receiver are resolvable. Details of Step 1 are given in Section B-B.
- *Step 2 (Constructing Precoding Vectors):* Based on the precoding vector assignment and the IA scheme in Step 1, we propose an approach to construct the precoding vectors at the transmitters. Specifically, we divide the precoding vectors into two groups: $\mathcal{U}^{\mathrm{basis}}$ and $\mathcal{U}^{\mathrm{algn}}$. For a precoding vector in $\mathcal{U}^{\mathrm{basis}}$, we let $\mathbf{u}_i^k := \mathbf{e}_k$. For the precoding vectors in $\mathcal{U}^{\mathrm{algn}}$, we construct them based on the IA scheme in Step 1. Details of Step 2 are given in Section B-C.
- *Step 3 (Existence of decoding vectors):* We show that the constructed precoding vectors in Step 2 satisfy (32) in Lemma 3. So we can conclude that DoF vector $\varphi = (z_1, z_2, \cdots, z_{N_{\mathrm{T}}})$ is feasible. Details of Step 3 are given in Section B-D.

B. Step 1: Precoding Vector Assignment and IA Scheme

Precoding Vector Assignment at a Transmitter. Consider transmitter i and one of its interfering receivers, say $j \in \mathcal{Q}_i$, as shown in Fig. 11. Receiver j is interfered with by z_i streams from transmitter i. Among these z_i interfering streams, our IA scheme must align α_{ij} interfering streams onto other interfering streams at receiver j.[5] As illustrated in the motivating example in Section III, in order to align α_{ij} interfering streams at receiver j, α_{ij} precoding vectors at transmitter i should be constructed to achieve this alignment. Denote $\mathcal{U}_{ij}^{\mathrm{algn}}$ as the set of precoding vectors in $\mathcal{U}_i$ that are used for aligning α_{ij} interfering streams at receiver $j \in \mathcal{Q}_i$. Then we have $|\mathcal{U}_{ij}^{\mathrm{algn}}| = \alpha_{ij}$ for $j \in \mathcal{Q}_i$. In other words, the precoding vectors in $\mathcal{U}_{ij}^{\mathrm{algn}}$ are constructed to align its corresponding α_{ij} interfering streams onto some other directions at receiver $j \in \mathcal{Q}_i$.

Based on (28), we have $\sum_{j \in \mathcal{Q}_i} \alpha_{ij} \leq z_i$, indicating that transmitter i has enough precoding vectors for IA at the receivers in $\mathcal{Q}_i$ (i.e., $\mathcal{U}_{ij_1}^{\mathrm{algn}} \cap \mathcal{U}_{ij_2}^{\mathrm{algn}} = \emptyset$ for $j_1, j_2 \in \mathcal{Q}_i$). Denote $\mathcal{U}_i^{\mathrm{basis}}$ as the set of precoding vectors in $\mathcal{U}_i$ that are not used for alignment at any receiver, i.e., $\mathcal{U}_i^{\mathrm{basis}} = \mathcal{U}_i \backslash (\cup_{j \in \mathcal{Q}_i} \mathcal{U}_{ij}^{\mathrm{algn}})$. Then we have $|\mathcal{U}_i^{\mathrm{basis}}| = z_i - \sum_{j \in \mathcal{Q}_i} \alpha_{ij}$. The precoding vector assignment for $\mathcal{U}_{ij}^{\mathrm{algn}}$ and $\mathcal{U}_i^{\mathrm{basis}}$ are shown in Fig. 11.

An IA Scheme at a Receiver. We now consider receiver j and its unintended transmitters in $\mathcal{P}_j$ as shown in Fig. 12. Our precoding vector assignment scheme ensures that α_{ij} interfering streams from transmitter $i \in \mathcal{P}_j$ can always be aligned to any directions (by constructing the precoding vectors in $\mathcal{U}_{ij}^{\mathrm{algn}}$). Now the question to ask is: For $i \in \mathcal{P}_j$, how do we align those α_{ij} interfering streams at receiver j? This question was answered in the proof of Lemma 1. We recap the IA scheme as follows. Recall $\mathcal{Z}_i$ is the set of interfering streams from transmitter i and $\mathcal{A}_{ij}$ consists of those α_{ij} interfering streams to be aligned. The IA scheme is to align each interfering stream in $\mathcal{A}_{ij}$ to a *unique* interfering stream in $\cup_{i' \in \mathcal{P}_j}^{i' \neq i} \mathcal{Z}_{i'} \backslash \mathcal{A}_{i'j}$. Based on (29), each interfering stream in $\mathcal{A}_{ij}$ can be successfully aligned to another interfering stream in this IA scheme.

[5] Receiver j in Fig. 11 is also interfered with by other unintended transmitters, which are not shown in the figure.

This article has been accepted for publication in a future issue of this journal, but has not been fully edited. Content may change prior to final publication. Citation information: DOI 10.1109/TVT.2018.2817365, IEEE Transactions on Vehicular Technology

Per our notation, the set of precoding vectors for the interfering streams in $\mathcal{A}_{ij}$ is $\mathcal{U}_{ij}^{\text{algn}}$ and the set of precoding vectors for the interfering streams in $\cup_{i'\in\mathcal{P}_j}^{i'\neq i}\mathcal{Z}_{i'}\backslash\mathcal{A}_{i'j}$ is $\cup_{i'\in\mathcal{P}_j}^{i'\neq i}\mathcal{U}_{i'}\backslash\mathcal{U}_{i'j}^{\text{algn}}$. To achieve our IA scheme, $\mathbf{u}_i^k \in \mathcal{U}_{ij}^{\text{algn}}$ should be constructed by $\mathbf{u}_i^k := \mathbf{H}_{ji}^{-1}\mathbf{H}_{ji'}\mathbf{u}_{i'}^{k'}$, where $\mathbf{u}_{i'}^{k'} \in \cup_{i'\in\mathcal{P}_j}^{i'\neq i}\mathcal{U}_{i'}\backslash\mathcal{U}_{i'j}^{\text{algn}}$. For simplicity, we denote $\mathbf{u}_i^k := \mathbf{H}_{ji}^{-1}\mathbf{H}_{ji'}\mathbf{u}_{i'}^{k'}$ as $\mathbf{u}_i^k \xrightarrow{j} \mathbf{u}_{i'}^{k'}$.

Denoting $\mathcal{U}_i^{\text{algn}} = \cup_{j\in\mathcal{Q}_i}\mathcal{U}_{ij}^{\text{algn}}$, we have the following lemma for transmitter $i = 1, 2, \cdots, N_{\text{T}}$.

Lemma 4: For each $\mathbf{u}_i^k \in \mathcal{U}_i^{\text{algn}}$, there exist a unique j and a unique $\mathbf{u}_{i'}^{k'}$, such that $\mathbf{u}_i^k \xrightarrow{j} \mathbf{u}_{i'}^{k'}$ with $i' \neq i$.

Lemma 4 is straightforward based on our precoding vector design and IA scheme. We omit the proof to conserve the space.

C. Step 2: Constructing Precoding Vectors

We now show how to construct the precoding vectors at each transmitter based on the IA scheme in Section B. Denote $\mathcal{U}$ as the set of all precoding vectors in the network, i.e., $\mathcal{U} = \bigcup_{i=1}^{N_{\text{T}}}\mathcal{U}_i$. Denote $\mathcal{U}^{\text{algn}}$ as the set of the precoding vectors used for alignment, i.e., $\mathcal{U}^{\text{algn}} = \bigcup_{i=1}^{N_{\text{T}}}\mathcal{U}_i^{\text{algn}}$. Denote $\mathcal{U}^{\text{basis}}$ as the set of the precoding vectors not used for alignment, i.e., $\mathcal{U}^{\text{basis}} = \bigcup_{i=1}^{N_{\text{T}}}\mathcal{U}_i^{\text{basis}}$. It should be noted that $\mathcal{U}^{\text{algn}}$ and $\mathcal{U}^{\text{basis}}$ are two disjoint sets and $\mathcal{U} = \mathcal{U}^{\text{algn}} \cup \mathcal{U}^{\text{basis}}$.

To construct the precoding vectors in $\mathcal{U}$, we first construct the precoding vectors in $\mathcal{U}^{\text{basis}}$ and then construct the precoding vectors in $\mathcal{U}^{\text{algn}}$. For each precoding vector in $\mathcal{U}^{\text{basis}}$, we let:

$$\mathbf{u}_i^k := \mathbf{e}_k, \qquad \text{for } \mathbf{u}_i^k \in \mathcal{U}^{\text{basis}}, \tag{34}$$

where $\mathbf{e}_k$ is a vector with 1 for the k-th element and 0 for all the others.

For the precoding vectors in $\mathcal{U}^{\text{algn}}$, their construction is more complicated, as we describe as follows. Based on Lemma 4, we know that if $\mathbf{u}_{i_1}^{k_1} \in \mathcal{U}^{\text{algn}}$, then there exists a precoding vector $\mathbf{u}_{i_2}^{k_2}$ such that $\mathbf{u}_{i_1}^{k_1} \xrightarrow{j_1} \mathbf{u}_{i_2}^{k_2}$ (i.e., $\mathbf{u}_{i_1}^{k_1} := \mathbf{H}_{j_1i_1}^{-1}\mathbf{H}_{j_1i_2}\mathbf{u}_{i_2}^{k_2}$). To construct $\mathbf{u}_{i_1}^{k_1}$, we first need to construct $\mathbf{u}_{i_2}^{k_2}$. If $\mathbf{u}_{i_2}^{k_2} \in \mathcal{U}^{\text{basis}}$, we know that $\mathbf{u}_{i_2}^{k_2}$ has already been constructed by (34). Otherwise (i.e., $\mathbf{u}_{i_2}^{k_2} \in \mathcal{U}^{\text{algn}}$), we construct $\mathbf{u}_{i_2}^{k_2}$ in the same way as $\mathbf{u}_{i_1}^{k_1}$, i.e., there exists a precoding vector $\mathbf{u}_{i_3}^{k_3}$ such that $\mathbf{u}_{i_2}^{k_2} \xrightarrow{j_2} \mathbf{u}_{i_3}^{k_3}$. Following the same token, we can establish a chain as follows:

$$\mathcal{C}: \mathbf{u}_{i_1}^{k_1} \xrightarrow{j_1} \mathbf{u}_{i_2}^{k_2} \xrightarrow{j_2} \cdots\cdots \xrightarrow{j_{M-2}} \mathbf{u}_{i_{M-1}}^{k_{M-1}} \xrightarrow{j_{M-1}} \mathbf{u}_{i_M}^{k_M}, \tag{35}$$

where $i_m \neq i_{m+1}$ for $m = 1, 2, \cdots, M-1$.

Chain $\mathcal{C}$ terminates if any of the following two cases occurs.

- *Case I:* $\mathbf{u}_{i_M}^{k_M}$ has already been constructed.
- *Case II:* $\mathbf{u}_{i_M}^{k_M}$ appears twice in chain $\mathcal{C}$.

It is easy to see that chain $\mathcal{C}$ will terminate, either by case I or case II. We now show how to construct the precoding vectors in chain $\mathcal{C}$ in each case, respectively.

Case I. In this case, chain $\mathcal{C}$ terminates because $\mathbf{u}_{i_M}^{k_M}$ has already been constructed. We can conclude: (i) all other precoding vectors in chain $\mathcal{C}$ have not been constructed; (ii) all precoding vectors in this chain are unique. Thus, we can construct the precoding vectors in chain $\mathcal{C}$ sequentially in the *backward* direction as follows:

$$\mathbf{u}_{i_{M-1}}^{k_{M-1}} := \mathbf{H}_{j_{M-1}i_{M-1}}^{-1}\mathbf{H}_{j_{M-1}i_M}\mathbf{u}_{i_M}^{k_M}.$$

After obtaining $\mathbf{u}_{i_{M-1}}^{k_{M-1}}$, we then construct $\mathbf{u}_{i_{M-2}}^{k_{M-2}}$ by

$$\mathbf{u}_{i_{M-2}}^{k_{M-2}} := \mathbf{H}_{j_{M-2}i_{M-2}}^{-1}\mathbf{H}_{j_{M-2}i_{M-1}}\mathbf{u}_{i_{M-1}}^{k_{M-1}}.$$

Following the same token, we construct all the precoding vectors in chain $\mathcal{C}$.

Case II. In this case, chain $\mathcal{C}$ terminates because $\mathbf{u}_{i_M}^{k_M}$ appears twice. We can conclude: (i) all precoding vectors in chain $\mathcal{C}$ have not been constructed; (ii) all precoding vectors in chain $\mathcal{C}$ are unique except $\mathbf{u}_{i_M}^{k_M}$; (iii) there exists $\hat{m}$ such that $(i_{\hat{m}}, k_{\hat{m}}) = (i_M, k_M)$ and $1 \leq \hat{m} < M$.

To construct the precoding vectors in chain $\mathcal{C}$, we divide chain $\mathcal{C}$ into two sub-chains $\mathcal{C}_1$ and $\mathcal{C}_2$:

$$\mathcal{C}_1: \mathbf{u}_{i_1}^{k_1} \xrightarrow{j_1} \mathbf{u}_{i_2}^{k_2} \xrightarrow{j_2} \cdots \xrightarrow{j_{\hat{m}-2}} \mathbf{u}_{i_{\hat{m}-1}}^{k_{\hat{m}-1}} \xrightarrow{j_{\hat{m}-1}} \mathbf{u}_{i_{\hat{m}}}^{k_{\hat{m}}},$$
$$\mathcal{C}_2: \mathbf{u}_{i_{\hat{m}}}^{k_{\hat{m}}} \xrightarrow{j_{\hat{m}}} \mathbf{u}_{i_{\hat{m}+1}}^{k_{\hat{m}+1}} \xrightarrow{j_{\hat{m}+1}} \cdots \xrightarrow{j_{M-2}} \mathbf{u}_{i_{M-1}}^{k_{M-1}} \xrightarrow{j_{M-1}} \mathbf{u}_{i_M}^{k_M},$$

where $(i_{\hat{m}}, k_{\hat{m}}) = (i_M, k_M)$.

For these two sub-chains, we first construct the precoding vectors in $\mathcal{C}_2$ and then construct the precoding vectors in $\mathcal{C}_1$. Based on the relationships among the vectors in chain $\mathcal{C}_2$, we have:

$$\begin{aligned}
\mathbf{u}_{i_{\hat{m}}}^{k_{\hat{m}}} &:= \mathbf{H}_{j_{\hat{m}}i_{\hat{m}}}^{-1}\mathbf{H}_{j_{\hat{m}}i_{\hat{m}+1}}\mathbf{u}_{i_{\hat{m}+1}}^{k_{\hat{m}+1}},\\
\mathbf{u}_{i_{\hat{m}+1}}^{k_{\hat{m}+1}} &:= \mathbf{H}_{j_{\hat{m}+1}i_{\hat{m}+1}}^{-1}\mathbf{H}_{j_{\hat{m}+1}i_{\hat{m}+2}}\mathbf{u}_{i_{\hat{m}+2}}^{k_{\hat{m}+2}},\\
&\vdots\\
\mathbf{u}_{i_{M-2}}^{k_{M-2}} &:= \mathbf{H}_{j_{M-2}i_{M-2}}^{-1}\mathbf{H}_{j_{M-2}i_{M-1}}\mathbf{u}_{i_{M-1}}^{k_{M-1}},\\
\mathbf{u}_{i_{M-1}}^{k_{M-1}} &:= \mathbf{H}_{j_{M-1}i_{M-1}}^{-1}\mathbf{H}_{j_{M-1}i_M}\mathbf{u}_{i_M}^{k_M}.
\end{aligned} \tag{36}$$

Given that $(i_{\hat{m}}, k_{\hat{m}}) = (i_M, k_M)$, we have

$$\mathbf{u}_{i_{\hat{m}}}^{k_{\hat{m}}} = \mathbf{u}_{i_M}^{k_M}. \tag{37}$$

(36) and (37) form a system of linear equations, where $\mathbf{H}$'s are given matricies and $\mathbf{u}$'s are variables. It can be verified that a solution to $\mathbf{u}_{i_M}^{k_M}$ in the system is

$$\mathbf{u}_{i_M}^{k_M} := \text{eigvec}\left(\prod_{m=\hat{m}}^{M-1}(\mathbf{H}_{j_mi_m}^{-1}\mathbf{H}_{j_mi_{m+1}})\right), \tag{38}$$

where $\text{eigvec}(\cdot)$ is an eigenvector of the square matrix. Once we obtain $\mathbf{u}_{i_M}^{k_M}$, we can sequentially construct all the other precoding vectors in sub-chain $\mathcal{C}_2$ by (36).

After constructing the precoding vectors in sub-chain $\mathcal{C}_2$, we construct the precoding vectors in sub-chain $\mathcal{C}_1$. Since $\mathbf{u}_{i_{\hat{m}}}^{k_{\hat{m}}}$ has already been constructed, we can construct the other precoding vectors in sub-chain $\mathcal{C}_1$ following the same token in Case I.

It is easy to see that all precoding vectors in $\mathcal{U}^{\text{algn}}$ are constructed at the end of the above procedure.

This article has been accepted for publication in a future issue of this journal, but has not been fully edited. Content may change prior to final publication. Citation information: DOI 10.1109/TVT.2018.2817365, IEEE Transactions on Vehicular Technology

D. Step 3: Existence of Decoding Vectors

We now show that the constructed precoding vectors in Step 2 satisfy (32) in Lemma 3. First, we present the following lemma.

Lemma 5: The constructed precoding vectors at each transmitter are linearly independent, i.e., $\dim(\mathcal{U}_i) = z_i$ *for* $1 \leq i \leq N_{\mathrm{T}}$.

Proof. Consider transmitter i in Fig. 11. Recall that set $\mathcal{U}_i$ is divided into two disjoint subsets: $\mathcal{U}_i^{\mathrm{algn}}$ and $\mathcal{U}_i^{\mathrm{basis}}$. Each precoding vector in $\mathcal{U}_i^{\mathrm{basis}}$ was constructed by letting $\mathbf{u}_i^k := \mathbf{e}_k$ and each precoding vector in $\mathcal{U}_i^{\mathrm{algn}}$ was constructed by $\mathbf{u}_i^k := \mathbf{H}_{ji}^{-1}\mathbf{H}_{ji'}\mathbf{u}_{i'}^{k'}$ (with $i \neq i'$). This indicates that the precoding vectors in $\mathcal{U}_i^{\mathrm{basis}}$ are independent of the channel matrices and the precoding vectors in $\mathcal{U}_i^{\mathrm{algn}}$ are dependent on the channel matrices. Given that the channel matrices are independent Gaussian random matrices, we have

$$\begin{aligned}\dim(\mathcal{U}_i) &= \dim(\mathcal{U}_i^{\mathrm{algn}} \cup \mathcal{U}_i^{\mathrm{basis}}) \\ &= \dim(\mathcal{U}_i^{\mathrm{algn}}) + \dim(\mathcal{U}_i^{\mathrm{basis}}) \\ &= \dim(\mathcal{U}_i^{\mathrm{algn}}) + |\mathcal{U}_i^{\mathrm{basis}}| \end{aligned} \tag{39}$$

almost surely.

Now we analyze the dimension of $\mathcal{U}_i^{\mathrm{algn}}$. Consider two precoding vectors $\mathbf{u}_i^k \in \mathcal{U}_{ij_1}^{\mathrm{algn}}$ and $\mathbf{u}_i^{k'} \in \mathcal{U}_{ij_2}^{\mathrm{algn}}$ with $j_1 \neq j_2$. In our precoding vector construction, $\mathbf{u}_i^k$ was constructed by letting $\mathbf{u}_i^k := \mathbf{H}_{j_1 i}^{-1}\mathbf{H}_{j_1 i_1}\mathbf{u}_{i_1}^{k_1}$ and $\mathbf{u}_i^{k'}$ was constructed by letting $\mathbf{u}_i^{k'} := \mathbf{H}_{j_2 i}^{-1}\mathbf{H}_{j_2 i_2}\mathbf{u}_{i_2}^{k_2}$ for some i_1, k_1, i_2, and k_2. Hence, $\mathbf{u}_i^k$ is dependent on $\mathbf{H}_{j_1 i}$, but $\mathbf{u}_i^{k'}$ is dependent on $\mathbf{H}_{j_2 i}$. Given that $\mathbf{H}_{j_1 i}$ and $\mathbf{H}_{j_2 i}$ are two independent Gaussian random matrices, we have

$$\dim(\mathcal{U}_i^{\mathrm{algn}}) = \dim(\bigcup_{j\in\mathcal{Q}_i} \mathcal{U}_{ij}^{\mathrm{algn}}) = \sum_{j\in\mathcal{Q}_i} \dim(\mathcal{U}_{ij}^{\mathrm{algn}}) \tag{40}$$

almost surely.

We now analyze the dimension of $\mathcal{U}_{ij}^{\mathrm{algn}}$. Based on (35), a precoding vector in $\mathcal{U}_{ij}^{\mathrm{algn}}$ is constructed in the following form:

$$\mathbf{u}_i^k = \left(\prod_{m=1}^{M-1} (\mathbf{H}_{j_m i_m}^{-1}\mathbf{H}_{j_m i_{m+1}})\right) \mathbf{u}_{i_M}^{k_M},$$

where $(i_1, k_1) = (i, k)$, $M \geq 2$, and $\mathbf{u}_{i_M}^{k_M}$ is constructed either by (34) or (38). Let $\mathbf{G}_i^k = \prod_{m=1}^{M-1}(\mathbf{H}_{j_m i_m}^{-1}\mathbf{H}_{j_m i_{m+1}})$. We call $\mathbf{G}_i^k$ the "effective channel" for $\mathbf{u}_i^k$. We divide the precoding vectors in $\mathcal{U}_{ij}^{\mathrm{algn}}$ into subsets such that the precoding vectors in the same subset have the same "effective channel". Denote the subsets as $\mathcal{U}_{ijn}^{\mathrm{algn}}$, $1 \leq n \leq N_{ij}$. Since $\mathbf{H}_{ij}$'s are independent Gaussian random matrices, any two "effective channels" are independent random matrices. Thus, we have

$$\dim(\mathcal{U}_{ij}^{\mathrm{algn}}) = \sum_{n=1}^{N_{ij}} \dim(\mathcal{U}_{ijn}^{\mathrm{algn}}). \tag{41}$$

For each $\mathbf{u}_i^k \in \mathcal{U}_{ijn}^{\mathrm{algn}}$, it is determined by its corresponding precoding vector $\mathbf{u}_{i_M}^{k_M}$ and $\mathbf{u}_{i_M}^{k_M}$ is constructed either by (34) or (38). Denote $\tilde{\mathcal{U}}_{ijn}^{\mathrm{algn}}$ as the set of precoding vectors $\mathbf{u}_{i_M}^{k_M}$ corresponding to the precoding vectors in $\mathcal{U}_{ijn}^{\mathrm{algn}}$. Then we have $\dim(\tilde{\mathcal{U}}_{ijn}^{\mathrm{algn}}) = |\tilde{\mathcal{U}}_{ijn}^{\mathrm{algn}}|$ based on three facts: (i) the precoding vectors in $\tilde{\mathcal{U}}_{ijn}^{\mathrm{algn}}$ are at the same transmitter; (ii) the precoding vectors constructed by (34) are linearly independent; (iii) there are A linearly independent solutions (eigenvectors) to (38). Thus, we have

$$\dim(\mathcal{U}_{ijn}^{\mathrm{algn}}) = \dim(\tilde{\mathcal{U}}_{ijn}^{\mathrm{algn}}) = |\tilde{\mathcal{U}}_{ijn}^{\mathrm{algn}}| = |\mathcal{U}_{ijn}^{\mathrm{algn}}|, \tag{42}$$

where the first equation follows from the fact that the "effective channel" has full rank.

Based on (41) and (42), we have

$$\dim(\mathcal{U}_{ij}^{\mathrm{algn}}) = \sum_{n=1}^{N_{ij}} \dim(\mathcal{U}_{ijn}^{\mathrm{algn}}) = \sum_{n=1}^{N_{ij}} |\mathcal{U}_{ijn}^{\mathrm{algn}}| = |\mathcal{U}_{ij}^{\mathrm{algn}}|. \tag{43}$$

Based on (39), (40), and (43), we have

$$\begin{aligned}\dim(\mathcal{U}_i) &= \dim(\mathcal{U}_i^{\mathrm{algn}}) + |\mathcal{U}_i^{\mathrm{basis}}| \\ &= \sum_{j\in\mathcal{Q}_i} \dim(\mathcal{U}_{ij}^{\mathrm{algn}}) + |\mathcal{U}_i^{\mathrm{basis}}| \\ &= \sum_{j\in\mathcal{Q}_i} |\mathcal{U}_{ij}^{\mathrm{algn}}| + |\mathcal{U}_i^{\mathrm{basis}}| \\ &= |\mathcal{U}_i^{\mathrm{algn}}| + |\mathcal{U}_i^{\mathrm{basis}}| \\ &= |\mathcal{U}_i| \\ &= z_i\ . \end{aligned}$$

Therefore, Lemma 5 is proved. □

Denote $\mathcal{D}_j^{\mathrm{I,eff}}$ as the set of "effective" interfering stream directions at receiver R_j. Denote $\mathcal{D}_j^{\mathrm{I,algn}}$ as the set of interfering stream directions for alignment at receiver R_j. Mathematically, we have

$$\begin{aligned}\mathcal{D}_j^{\mathrm{I,eff}} &= \bigcup_{i\in\mathcal{P}_j} \{\mathbf{H}_{ji}\mathbf{u}_i^k : \mathbf{u}_i^k \in \mathcal{U}_i \backslash \mathcal{U}_{ij}^{\mathrm{algn}}\}, \\ \mathcal{D}_j^{\mathrm{I,algn}} &= \bigcup_{i\in\mathcal{P}_j} \{\mathbf{H}_{ji}\mathbf{u}_i^k : \mathbf{u}_i^k \in \mathcal{U}_{ij}^{\mathrm{algn}}\}. \end{aligned}$$

Based on our procedure to construct the precoding vector construction procedure, we know that for each $\mathbf{H}_{ji}\mathbf{u}_i^k \in \mathcal{D}_j^{\mathrm{I,algn}}$, there exists a $\mathbf{H}_{ji'}\mathbf{u}_{i'}^{k'} \in \mathcal{D}_j^{\mathrm{I,eff}}$ such that $\mathbf{H}_{ji}\mathbf{u}_i^k := \mathbf{H}_{ji'}\mathbf{u}_{i'}^{k'}$. Thus we have

$$\mathrm{span}(\mathcal{D}_j^{\mathrm{I,algn}}) \subseteq \mathrm{span}(\mathcal{D}_j^{\mathrm{I,eff}}). \tag{44}$$

For the number of vectors in $\mathcal{D}_j^{\mathrm{S}} \cup \mathcal{D}_j^{\mathrm{I,eff}}$, we have

$$|\mathcal{D}_j^{\mathrm{S}} \cup \mathcal{D}_j^{\mathrm{I,eff}}| \leq \sum_{i\in\mathcal{T}_j} z_i + \sum_{i\in\mathcal{P}_j} (z_i - \alpha_{ij}) \leq A, \tag{45}$$

where the first inequality follows from our definitions and the second inequality follows from (30).

This article has been accepted for publication in a future issue of this journal, but has not been fully edited. Content may change prior to final publication. Citation information: DOI 10.1109/TVT.2018.2817365, IEEE Transactions on Vehicular Technology

The dimension of signal and interference space at receiver j can be written as:

$$\begin{aligned}\dim(\mathcal{D}_j^{\mathrm{S}} \cup \mathcal{D}_j^{\mathrm{I}}) &\overset{(a)}{=} \dim(\mathcal{D}_j^{\mathrm{S}} \cup \mathcal{D}_j^{\mathrm{I,eff}}) \\ &\overset{(b)}{=} \dim(\mathcal{D}_j^{\mathrm{S}}) + \dim(\mathcal{D}_j^{\mathrm{I,eff}}) \\ &\overset{(c)}{=} \dim \cup_{i\in\mathcal{T}_j} \{\mathbf{H}_{ji}\mathbf{u}_i^k : \mathbf{u}_i^k \in \mathcal{U}_i\} + \\ &\quad \dim \cup_{i\in\mathcal{P}_j} \{\mathbf{H}_{ji}\mathbf{u}_i^k : \mathbf{u}_i^k \in \mathcal{U}_i \backslash \mathcal{U}_{ij}^{\mathrm{algn}}\} \\ &\overset{(d)}{=} \dim \cup_{i\in\mathcal{T}_j} \{\mathcal{U}_i\} + \dim \cup_{i\in\mathcal{P}_j} \{\mathcal{U}_i \backslash \mathcal{U}_{ij}^{\mathrm{algn}}\} \\ &\overset{(e)}{=} \sum_{i\in\mathcal{T}_j} \dim\{\mathcal{U}_i\} + \sum_{i\in\mathcal{P}_j} \dim\{\mathcal{U}_i \backslash \mathcal{U}_{ij}^{\mathrm{algn}}\} \\ &\overset{(f)}{=} \sum_{i\in\mathcal{T}_j} |\mathcal{U}_i| + \sum_{i\in\mathcal{P}_j} |\mathcal{U}_i \backslash \mathcal{U}_{ij}^{\mathrm{algn}}| \\ &\overset{(g)}{=} \sum_{i\in\mathcal{T}_j} z_i + \sum_{i\in\mathcal{P}_j} (z_i - \alpha_{ij}), \end{aligned} \tag{46}$$

where (a) follows from (44); (b) follows since (i) $\mathcal{T}_j$ and $\mathcal{P}_j$ are disjoint sets (i.e., $\mathcal{T}_j \cap \mathcal{P}_j = \emptyset$), (ii) the number of elements in $\mathcal{D}_j^{\mathrm{S}} \cup \mathcal{D}_j^{\mathrm{I,eff}}$ is upper bounded by A as shown in (45), and (iii) $\mathbf{H}_{ji}$ is independent Gaussian random matrix for each channel; (c) follows from our definitions of $\mathcal{D}_j^{\mathrm{S}}$ and $\mathcal{D}_j^{\mathrm{I,eff}}$; (d) follows from our assumption that $\mathbf{H}_{ji}$ has full rank; (e) follows since $\mathbf{H}_{ji}$ is independent Gaussian random matrix for each channel; (f) follows from Lemma 5; (g) follows from the definitions of $\mathcal{U}_i$ and $\mathcal{U}_i^{\mathrm{algn}}$.

Similarly, the dimension of interference subspace at receiver j can be written as:

$$\dim(\mathcal{D}_j^{\mathrm{I}}) = \dim(\mathcal{D}_j^{\mathrm{I,eff}}) = \sum_{i\in\mathcal{P}_j} (z_i - \alpha_{ij}). \tag{47}$$

Based on (46) and (47), we have

$$\dim(\mathcal{D}_j^{\mathrm{S}} \cup \mathcal{D}_j^{\mathrm{I}}) = \sum_{i\in\mathcal{T}_j} z_i + \dim(\mathcal{D}_j^{\mathrm{I}}), \tag{48}$$

which indicates that the constructed precoding vectors meet (32) in Lemma 3. This completes our proof.

Appendix C
Proof of Theorem 2

We prove this theorem in two steps.

Step 1. We prove $(1-\varepsilon)\cdot r_{\min}^*(\mathrm{MTM}_2) \le r_{\min}^*(\mathrm{MTM}_3)$ by showing that if $r_{\min}$ is the optimal objective value of MTM_2, then $(1-\varepsilon)r_{\min}$ is an achievable objective value of MTM_3. Suppose that $r_{\min}$ is the optimal objective value of MTM_2, i.e., $r_{\min} = r_{\min}^*(\mathrm{MTM}_2)$. Then its corresponding solution $\varphi = [r_{\min}, r(f), c_i(t), c_i^k(t), \gamma_{ij}^k(t), other\_variables]$ is obviously feasible and satisfies all the constraints in MTM_2. Based on φ, we construct a solution $\hat{\varphi}$ to MTM_3 as follows:

$$\hat{\varphi} = \big[(1-\varepsilon)r_{\min}, (1-\varepsilon)r(f), (1-\varepsilon)c_i(t), (1-\varepsilon)c_i^k(t), \gamma_{ij}^k(t), other\_variables\big].$$

We now show that $\hat{\varphi}$ is a feasible solution to MTM_3. Since φ satisfies (3)–(8), (12)–(18), and (22)–(24), it is not difficult to verify that $\hat{\varphi}$ also satisfies these constraints. Since φ satisfies (25) in MTM_2, we have $W\log_2\left(1+\gamma_{ij}^k(t)\right) \ge c_i^k(t)$. Based on Alg. 1, we know that $D_m\gamma_{ij}^k(t)+E_m \ge (1-\varepsilon)\log_2(1+\gamma_{ij}^k(t))$ holds for $m = 1, 2, \cdots, M$. So we have $W\big(D_m\gamma_{ij}^k(t) + E_m\big) \ge (1-\varepsilon)c_i^k(t)$ for $m = 1, 2, \cdots, M$. This shows that $\hat{\varphi}$ satisfies (27). Since $\hat{\varphi}$ satisfies all the constraints in MTM_3, $\hat{\varphi}$ is a feasible solution to MTM_3 and its corresponding objective value is $(1-\varepsilon)r_{\min}$. So $(1-\varepsilon)r_{\min}$ is an achievable objective value of MTM_3 and $(1-\varepsilon)\cdot r_{\min}^*(\mathrm{MTM}_2) \le r_{\min}^*(\mathrm{MTM}_3)$ holds.

Step 2. We prove $r_{\min}^*(\mathrm{MTM}_3) \le r_{\min}^*(\mathrm{MTM}_2)$ by showing that if $r_{\min}$ is the optimal objective value of MTM_3, then $r_{\min}$ is an achievable objective value of MTM_2. Suppose that $r_{\min}$ is the optimal objective value of MTM_3, i.e., $r_{\min} = r_{\min}^*(\mathrm{MTM}_3)$. Then its corresponding solution $\varphi = [r_{\min}, r(f), c_i(t), c_i^k(t), \gamma_{ij}^k(t), other\_variables]$ is obviously feasible and satisfies all the constraints in MTM_3.

We now show that φ is a feasible solution to MTM_2. Since φ is a feasible solution to MTM_3, then φ satisfies (3)–(8), (12)–(18), (22)–(24), and (27). Since φ satisfies (27), we have $c_i^k(t) \le W\big(D_m\gamma_{ij}^k(t) + E_m\big)$ for $m = 1, 2, \cdots, M$. Based on Alg. 1, we know that $D_m\gamma_{ij}^k(t)+E_m \le \log_2(1+\gamma_{ij}^k(t))$ holds for some m. We have $c_i^k(t) \le W\cdot\log_2\left(1+\gamma_{ij}^k(t)\right)$. This indicates that φ satisfies (25). Since φ satisfies all the constraints in MTM_2, φ is a feasible solution to MTM_2 and its corresponding objective value is $r_{\min}$. So $r_{\min}$ is an achievable objective value of MTM_2. Therefore, $r_{\min}^*(\mathrm{MTM}_3) \le r_{\min}^*(\mathrm{MTM}_2)$ holds.

Appendix D
Problem Formulation Without IA

We formulate the same network throughput optimization problem without IA (but still with IC) as follows.

IC Constraints. Referring to Fig. 4, consider a node $k \in \mathcal{N}$. If $y_k(t) = 1$ (i.e., node j is a receiver), then the number of its desired data streams is $\sum_{m\in\mathcal{T}_k} z_m(t)$ and the number of its interfering directions is $\sum_{i\in\mathcal{P}_k} z_i(t)$. To ensure resolvability of its desired data streams at node k, we must have: $\sum_{m\in\mathcal{T}_k} z_m(t) + \sum_{i\in\mathcal{P}_k} z_i(t) \le A$. Otherwise (i.e. $y_k(t) = 0$), there is no restriction on the number of the interfering directions at node k. Combining the two cases, we have:

$$\sum_{m\in\mathcal{T}_k} z_m(t) + \sum_{i\in\mathcal{P}_k} z_i(t) \le A + [1 - y_k(t)]\cdot B, \quad 1 \le k \le N, 1 \le t \le T\,. \tag{49}$$

Following the same token of formulating MTM_1 in Section IV, we can formulate the multicast throughput maximization problem without IA, denoted as MTM-noIA$_{\mathrm{raw}}$, as follows:

MTM-noIA$_{\mathrm{raw}}$

max $r_{\min}$

s.t. Multicast IC constraints: (49);
Multicast node constraints: (6)–(8);
One-hop multicast rate constraints: (9)–(11);
Multicast capacity constraints: (12)–(13).

This article has been accepted for publication in a future issue of this journal, but has not been fully edited. Content may change prior to final publication. Citation information: DOI 10.1109/TVT.2018.2817365, IEEE Transactions on Vehicular Technology

MTM-noIA$_{\rm raw}$ includes nonlinear constraints and thus falls in the category of MINLP. By following the linearization techniques in Section V, MTM-noIA$^{\rm raw}$ can be linearized to MTM-noIA:

MTM-noIA

max $r_{\min}$

s.t. Multicast IC constraints: (49);
Multicast node constraints: (6)–(8);
Multicast capacity constraints: (12)–(13);
One-hop multicast rate constraints: (14)–(18), (22)–(24), (27).

All the constraints in MTM-noIA are linear and thus MTM-noIA falls in the category of MILP. Based on the analysis in Section V, the optimal objective value of MTM-noIA is within $(1-\varepsilon)$-optimal of the objective value of MTM-noIA$_{\rm raw}$, i.e., $(1-\varepsilon)\cdot r^*_{\min}(\text{MTM-noIA}_{\rm raw}) \le r^*_{\min}(\text{MTM-noIA}) \le r^*_{\min}(\text{MTM-noIA}_{\rm raw})$.

REFERENCES

[1] V. R. Cadambe and S. A. Jafar, "Interference alignment and degrees of freedom of the K-user interference channel," *IEEE Trans. on Information Theory,* vol. 54, no. 8, pp. 3425–3441, Aug. 2008.

[2] S. Gollakotta, S. Perli, and D. Katabi, "Interference alignment and cancellation," in *Proc. of ACM SIGCOMM,* vol. 39 no. 4, pp. 159–170, Barcelona, Spain, Oct. 2009.

[3] O. El Ayach, S. W. Peters, and R. W. Heath, "The feasibility of interference alignment over measured MIMO-OFDM channels," *IEEE Trans. on Vehicular Technology,* vol. 59, no. 9, pp. 4309–4321, Nov. 2010.

[4] G. Bresler, D. Cartwright, and D. Tse, Feasibility of interference alignment for the MIMO interference channel. IEEE Transactions on Information Theory, vol. 60, no. 9, pp. 5573–5586, 2014.

[5] S. A. Jafar and S. Shamai, "Degrees of freedom region for the MIMO X channel," *IEEE Trans. on Information Theory,* vol. 54, no. 1, pp. 151–170, Jan. 2008.

[6] T. Gou and S. A. Jafar, "Degrees of freedom of the K user $M \times N$ MIMO interference channel," *IEEE Trans. on Information Theory,* vol. 56, no. 12, pp. 6040–6057, Dec. 2010.

[7] V. R. Cadambe and S. A. Jafar, "Interference alignment and the degrees of freedom of wireless X networks," *IEEE Trans. on Information Theory,* vol. 55, no. 9, pp. 3893–3908, Sept. 2009.

[8] N. Lee, J. B. Lim, and J. Chun, "Degrees of freedom of the MIMO Y channel: Signal space alignment for network coding," *IEEE Trans. on Information Theory,* vol. 56, no. 7, pp. 3332–3342, July 2010.

[9] S. A. Jafar, "The ergodic capacity of phase-fading interference networks," *IEEE Trans. Information Theory,* vol. 57, no. 12, pp. 7685–7694, Dec. 2011.

[10] C. Suh, M. Ho, and D. Tse, "Downlink interference alignment," *IEEE Trans. on Communications,* vol. 59, no. 9, pp. 2616–2626, Sept. 2011.

[11] H. J. Yang, W. Y. Shin, B. C. Jung, C. Suh, and A. Paulraj, "Opportunistic downlink interference alignment for multi-cell MIMO networks," *IEEE Transactions on Wireless Communications*, vol. 16, no. 3, pp. 1533–1548, Mar. 2017.

[12] M. Morales-Cespedes, J. Plata-Chaves, D. Toumpakaris, S. A. Jafar, and A. Garcia, "Blind interference alignment for cellular networks," *IEEE Transactions on Signal Processing,* vol. 63, no. 1, pp. 41–56, Jan. 2015.

[13] V. Ntranos, M. A. Maddah-Ali, and G. Caire, "Cellular interference alignment," *IEEE Transactions on Information Theory,* vol. 61, no. 3, pp. 1194–1217, Mar. 2015.

[14] C. M. Yetis, J. Fanjul, J. A. Garcia-Naya, N. N. Moghadam, and H. Farhadi, "Interference alignment testbeds," IEEE Communications Magazine, vol. 55, no. 10, pp. 120–126, Oct. 2017.

[15] L. E. Li, R. Alimi, D. Shen, H. Viswanathan, and Y. R. Yang, "A general algorithm for interference alignment and cancellation in wireless networks," in *Proc. of IEEE INFOCOM,* pp. 1774–1782, San Diego, CA, March 2010.

[16] A. Abdel-Hadi and S. Vishwanath, "On multicast interference alignment in multihop systems," in *Proc. IEEE Information Theory Workshop,* Cairo, Egypt, Jan. 2010.

[17] T. Gou, S. A. Jafar, C. Wang, S. W. Jeon, and S. Y. Chung, "Aligned interference neutralization and the degrees of freedom of the $2\times 2\times 2$ interference channel," *IEEE Trans. on Information Theory,* vol. 58, no. 7, pp. 4381–4395, July 2012.

[18] H. Zeng, Y. Shi, Y. T. Hou, W. Lou, S. Kompella, and S. F. Midkiff, "On interference alignment for multi-hop MIMO networks," in *Proc. of IEEE INFOCOM,* pp. 1330–1338, Turin, Italy, April 2013.

[19] H. Zeng, F. Tian, Y. T. Hou, W. Lou, and S. F. Midkiff, "Interference alignment for multihop wireless networks: challenges and research directions, *IEEE network*, vol. 30, no. 2, pp. 74–80, Mar./Apr. 2016.

[20] W. Ge, J. Zhang, and S. Shen, "A cross-layer design approach to multicast in wireless networks," *IEEE Trans. on Wireless Communications,* vol. 6, no. 3, pp. 1063–1071, March 2007.

[21] J. Xu, S. J. Lee, W. S. Kang, and J. S. Seo "Adaptive resource allocation for MIMO-OFDM based wireless multicast systems," *IEEE Trans. on Broadcasting,* vol. 56, no. 1, pp. 98–102, March 2010.

[22] F. Jiang; J. Wang; and A. L. Swindlehurst, "Interference-aware scheduling for connectivity in MIMO ad hoc multicast networks," *IEEE Trans. on Vehicular Technology,* vol. 61, no. 4, May 2012.

[23] X. Rao and V. K. N. Lau. "Minimization of CSI feedback dimension for interference alignment in MIMO interference multicast networks," *IEEE Trans. on Information Theory,* vol. 61, no. 3, pp. 1218–1246, March 2015.

[24] C. Gao, Y. Shi, Y. T. Hou, H. D. Sherali, and H. Zhou. "Multicast communications in multi-hop cognitive radio networks," *IEEE Journal on Selected Areas in Communications,* vol. 29, no. 4, pp. 784–793, April 2011.

[25] D. Ferguson, J. Moy, A. Lindem, *Open Shortest Path First (OSPF) for IPv6,* IETF, RFC 5340, July 2008.

[26] Y. T. Hou, Y. Shi, and H. D. Sherali, *Applied Optimization Methods for Wireless Networks,* Cambridge University Press, ISBN-13: 978-1107018808, April 2014.

[27] S. Sharma, Y. Shi, Y. T. Hou, H. D. Sherali, and S. Kompella, "Joint optimization of session grouping and relay node selection for network-coded cooperative communications," *IEEE Trans. on Mobile Computing,* vol. 13, no. 9, pp. 2028–2041, Sept. 2014

[28] IBM ILOG CPLEX Optimizer, software available at http://www-01.ibm.com/software/integration/optimization/cplex-optimizer.

[29] Y. Shi, Y. T. Hou, J. Liu, and S. Kompella, "Bridging the gap between protocol and physical models for wireless networks," *IEEE Trans. on Mobile Computing,* vol. 12, no. 7, pp. 1404–1416, July 2013.

[30] A. El-Gamal, and Y.-H. Kim. *Network Information Theory,* Cambridge University Press, 2011.

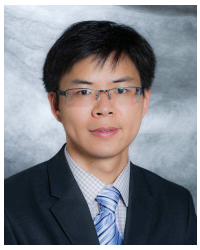

Huacheng Zeng (M'15) is an Assistant Professor of Electrical and Computer Engineering at University of Louisville, Louisville, KY. He received his Ph.D. degree in Computer Engineering from Virginia Tech, Blacksburg, VA, in 2015. He worked as a senior system engineering with Marvell Semiconductor, Inc. from 2015 to 2016. His research focuses on wireless communication system design and implementations.

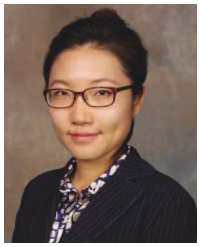

Xiaoqi Qin (M'16) received her B.S., M.S., and Ph.D. degree from Bradley Department of Electrical and Computer Engineering at Virginia Tech in 2011, 2013 and 2016, respectively. She is currently a lecturer in School of Information and Communication Engineering in Beijing University of Posts and Telecommunications in China. Her research interests include algorithm design and cross-layer optimization in wireless networks, coexistence and spectrum sharing in cognitive radio networks, and intelligent Internet of things.

This article has been accepted for publication in a future issue of this journal, but has not been fully edited. Content may change prior to final publication. Citation information: DOI 10.1109/TVT.2018.2817365, IEEE Transactions on Vehicular Technology

Xu Yuan (S'13–M'16) received the B.S. degree from the Department of Information Security, Nankai University, in 2009, and the Ph.D. degree from the Bradley Department of Electrical and Computer Engineering, Virginia Tech, Blacksburg, VA, USA, in 2016. From 2016 to 2017, he was a Post-Doctoral Fellow of Electrical and Computer Engineering with the University of Toronto, Toronto, ON, Canada. He is currently an Assistant Professor in the School of Computing and Informatics at the University of Louisiana at Lafayette, LA, USA. His research interest focuses on cloud computing security, algorithm design and optimization for spectrum sharing, coexistence, and cognitive radio networks.

Feng Tian (M'13) received the Ph.D. degree in signal and information processing from Nanjing University of Posts and Telecommunications, Nanjing, China, in 2008. He was a Visiting Scholar with Virginia Polytechnic Institute and State University, Blacksburg, VA, USA, from 2013 to 2015. He is currently an Associate Professor with Nanjing University of Posts and Telecommunications, China. His research focuses on performance optimization and algorithm design for wireless networks.

Y. Thomas Hou (F'14) is Bradley Distinguished Professor of Electrical and Computer Engineering at Virginia Tech, Blacksburg, VA, USA, which he joined in 2002. During 1997 to 2002, he was a Member of Research Staff at Fujitsu Laboratories of America, Sunnyvale, CA, USA. He received his Ph.D. degree from NYU Tandon School of Engineering in 1998. His current research focuses on developing innovative solutions to complex science and engineering problems arising from wireless and mobile networks. He has published over 100 journal papers and 130 conference papers in networking related areas. His papers were recognized by five best paper awards from the IEEE and two paper awards from the ACM. He holds five U.S. patents. He authored/co-authored two graduate textbooks: *Applied Optimization Methods for Wireless Networks* (Cambridge University Press, 2014) and *Cognitive Radio Communications and Networks: Principles and Practices* (Academic Press/Elsevier, 2009). He was/is on the editorial boards of a number of IEEE and ACM transactions and journals. He is the Steering Committee Chair of IEEE INFOCOM conference and a member of the IEEE Communications Society Board of Governors. He is also a Distinguished Lecturer of the IEEE Communications Society.

Wenjing Lou (F'15) is a Professor of Computer Science at Virginia Tech and a Fellow of the IEEE. She holds a Ph.D. in Electrical and Computer Engineering from the University of Florida. Her research interests cover many topics in the cybersecurity field, with her current research interest focusing on privacy protection techniques in networked information systems and cross-layer security enhancement in wireless networks. Prof. Lou is currently on the editorial boards of ACM/IEEE Transactions on Networking, IEEE Transactions on Mobile Computing, and Journal of Computer Security. She is the Steering Committee Chair of IEEE Conference on Communications and Network Security (IEEE CNS). She served as a program director at the US National Science Foundation (NSF) from 2014 to 2017.

Scott F. Midkiff (S'82–M'85–SM'92) is Professor & Vice President for Information Technology and Chief Information Officer at Virginia Tech, Blacksburg, VA. From 2009 to 2012, Prof. Midkiff was the Department Head of the Bradley Department of Electrical and Computer Engineering at Virginia Tech. From 2006 to 2009, he served as a program director at the National Science Foundation. Prof. Midkiff's research interests include wireless and ad hoc networks, network services for pervasive computing, and cyber-physical systems.